QIAN, HONG, M.S. Chloride Requirement in Photosystem II and Anion Effects in the S_2' State of the Oxygen Evolving Complex. (2006)
Directed by Dr. Alice Haddy. 66pp.

The oxygen evolving complex (OEC) of photosystem II (PSII) requires chloride as a critical cofactor. The Cl^- content of PSII was determined to be 1 Cl^-/PSII by the AgCl colloid assay. The dissociation constant for Cl^- in NaCl-washed PSII was determined using the Cl^- sensitive microelectrode. Two classes of Cl^- binding sites were found with K_d values of 53 μM and 4.2 mM.

The effects of anions on the S_2' oxidation state of the OEC were investigated using electron paramagnetic resonance spectroscopy. It was found that chloride was required for the formation of the S_2' state. The effect of iodide, which is an activator of oxygen evolution at low concentrations and an inhibitor at high concentrations, was also tested. Both low and high concentrations of I^- supported the formation of the S_2' state, suggesting that I^- inhibition occurs in some state higher than the S_2' state.

CHLORIDE REQUIREMENT IN PHOTOSYSTEM II AND ANION EFFECTS IN THE S_2' STATE OF THE OXYGEN EVOLVING COMPLEX

By

Hong Qian

A Thesis Submitted to
The Faculty of The Graduate School at
The University of North Carolina at Greensboro
In Partial Fulfillment
of the Requirements for the Degree
Master of Science

Greensboro
2006

Approved by

_____
Committee Chair

APPROVAL PAGE

This thesis has been approved by the following committee of the

Faculty of the Graduate School at the University of North Carolina at Greensboro.

Committee Chair _____

Committee Members _____

_____

_____
Date of Acceptance by Committee

_____
Date of Final Oral Examination

ACKNOWLEDGEMENTS

This research was founded by grants from the National Science Foundation and the Dreyfus Foundation.

I wish to thank Dr. Alice Haddy who performed the EPR spectroscopy on all of the samples recorded in this thesis.

This work is dedicated to Dr. Alice Haddy and my family.

TABLE OF CONTENTS

Page

CHAPTER I

INTRODUCTION

Photosynthesis is the process in which sunlight energy is converted to usable chemical energy by plants and some bacteria, producing fuel for all living things and oxygen as a byproduct. One of the centers of light absorption is photosystem II (PSII) which consists of a complex set of polypeptides, an oxygen-evolving complex (OEC), and electron transfer components. The OEC, containing a Mn cluster along with two essential cofactors, Ca^{2+} and Cl^-, and a nearby tyrosine residue (Y_z), cycles through five redox states, designated S_0 to S_4. Oxygen is released during the advancement from the S_4 to the S_0 state. Chloride has been known to be required for high rates of oxygen evolution, and the binding site of chloride is in close proximity to the manganese cluster. Chloride binding in other proteins such as peroxidases and hemoglobin has also been found, but full characterization of chloride binding in these proteins is still yet to be done. This thesis presents an investigation of the Cl^- requirement of PSII and anion effects on the newly discovered S_2' state, which includes determination of the amount of bound Cl^-, the Cl^- binding affinity in salt-washed PSII, and Cl^-/I^- effects on the S_2' state. In addition, several analytical methods for determining the amount of Cl^- in PSII was examined.

1. Background Information

a. Overview of Photosynthesis

Four billions years ago, some unicellular organisms developed the ability to use light from the sun as an energy source. By combining light energy and available sources of chemicals, these organisms evolved into the first photosynthetic species. The term "photosynthesis" is associated with this ability (1). Two to three billion years ago, a photosynthetic reaction center evolved which was capable of extracting electrons from water and releasing oxygen as a byproduct (2). For this reason alone, it is not surprising that understanding O_2 production by plants and other photosynthetic organisms has long been a focus of research in photosynthesis. Chloroplasts in plants are the subcellular organelle in which photosynthesis takes place. The overall reaction can be described as follows:

$$CO_2 + H_2O \rightarrow CH_2O + O_2$$

Actually photosynthesis is a multi-step process which can be divided into light reactions and dark reactions. Light reactions use light energy to oxidize H_2O, at the same time generating NADPH and a proton gradient. Dark reactions, which are light independent, use NADPH and ATP to drive the synthesis of carbohydrate.

Chlorophyll, which is found in the thylakoid membranes of chloroplasts, is used to harvest light and transfer light energy. Once harvested, the light energy is relayed to the reaction centers of photosystem I (PS I) and photosystem II (PS II), where the light reactions take place. PS II is directly involved in oxygen generation.

Understanding O_2 production in photosynthesis involves understanding both the structure and the function of the PS II protein complex. Although there are still many unanswered questions with regard to both the structure and the function of the

PS II, a model of PSII has been made according the information obtained so far (Figure 1). When light is absorbed by the chlorophyll in PS II, the light energy is trapped by initiation of a charge-separation reaction. This charge separation occurs at a special pair of chlorophyll called P680. Rapid electron transfer from the excited state P680* to an adjacent pheophytin is followed by slower electron transfer to a

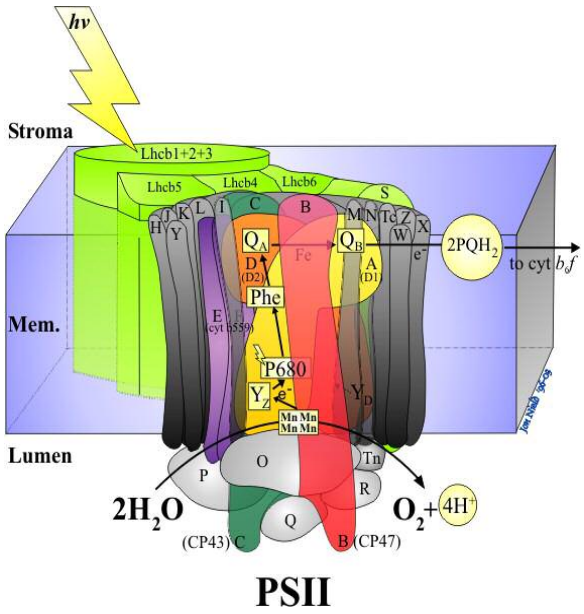

Figure. 1. Enlarged view of higher plant PS II
Taken from website of http://www.bio.ic.ac.uk/research/barber/psIIimages/PSII.html (Ref. 3)

bound plastoquinone, Q_A, forming the semiquinone radical anion Q_A^-. The electron is then transferred to another plastoquinone, Q_B, which is mobile. As the quinone at the Q_B site accepts two electrons, it takes two protons from the stromal side to become the hydroquinone form QH_2. Q_B leaves its site, transferring electrons to the next protein complex, and is replaced by a new quinone. The $P680^+$ chlorophyll cation formed by the initial electron transfer is a strong oxidant which rapidly oxidizes a nearby tyrosine, designated Y_z. Although $P680^+$ removes one electron from Y_z, Y_z also loses one proton at this step, forming a neutral radical $Y_z^{\cdot}$. Tyrosine then takes

an electron and a proton from the manganese cluster and/or another amino acid residue of the OEC. To replace its lost electrons and protons, the OEC strips electrons and protons away from H_2O, and then O_2 is released.

The OEC is therefore the site at which water binds and is oxidized to oxygen. The OEC, with its core of four Mn ions, Ca^{2+} and Cl^-, accumulates the energy needed to oxidize water to oxygen, as it transfers electrons to P680. After water is oxidized to oxygen, the OEC resets to its most reduced state.

To understand whether the conversion of water to oxygen happens in one step or in several, Joliot *et al* devised an experiment to deliver light flashes to a sample and then monitor the amount of oxygen after each flash. The experiment showed that oxygen was produced in cycles of 4 flashes (Figure 2) (2).

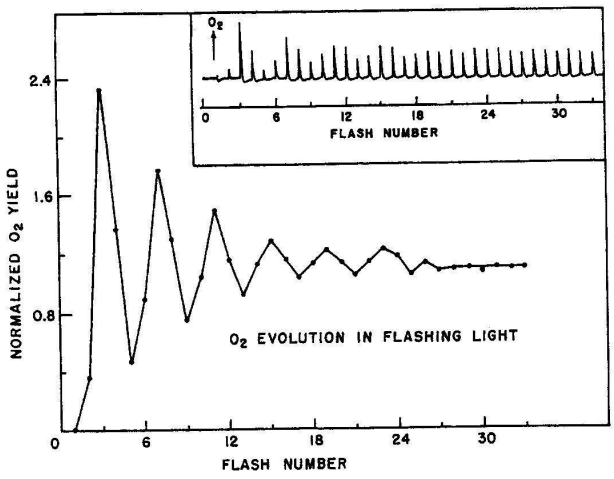

Figure 2. The amplitude of molecular oxygen released during a train of 21 μs saturating light flashes applied at 1 s intervals to a dark-adapted spinach chloroplast suspension (Babcock,1973). The inset shows kinetically resolved O_2 evolution traces, while the main plot displays amplitudes vs. flash number (Ref. 2)

Based on Joliot's experiment, Kok proposed five so-called S-states to model the oxygen evolution cycle. Each state is a storage state that PSII uses to accumulate oxidizing power. The S-state transitions represent single electron oxidations of the

Mn cluster in the OEC (Figure 3) (4). This means that the advancement from one S state to the next requires the removal of an electron from the Mn ions in the OEC and the absorption of a photon of light at the reaction center. During one full cycle, two water molecules bind to the OEC and are converted to reactive species so that by the end of the cycle O_2 is produced.

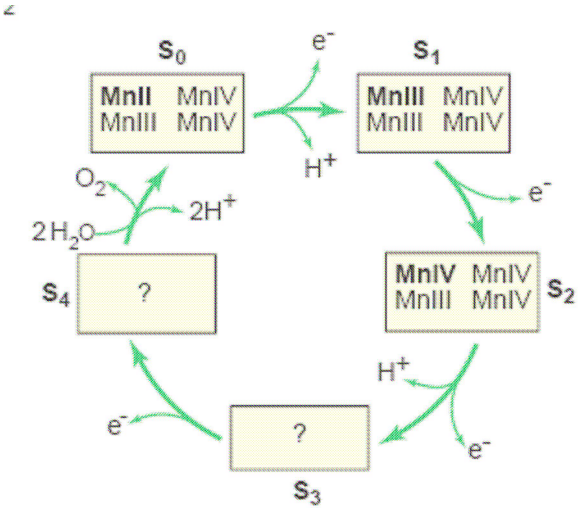

Figure 3. Kok S-state cycle (taken from Rutherford, 2003 (4)). The valence of Mn ions increases on the S_0 to S_1 to S_2 steps; however, this is less certain for the S_2 to S_3 to S_4 steps

b. Main subunits of PS II

At present there are 25 genes that have been identified as encoding proteins for the PSII core. These are referred to as *psb* (photosystem b) genes (3). In higher plants and algae, most of these genes are located in the chloroplast genome, but some are nuclear encoded. There are undoubtedly more to be discovered.

A summary in Table 1 gives the properties of the *psb* genes and their origins. In higher plants, at least six intrinsic proteins are required for oxygen evolution by PS II. These are CP47, CP43, the D1 and D2 proteins, and the α and β subunits of cytochrome b559. CP47 and CP43 serve as the proximal antennae for PS II, providing a conduit for excitation energy transfer from the exterior antennae of the

Table 1. Summary of the properties of *psb* genes and their origins

Protein	Subunit	Mass (kDa)	No. of transmembrane α-helices
PsbA (c)	Dl	38.021 (S)	5
PsbB (c)	CP47	56.278 (S)	6
PsbC (c)	CP43	50.066 (S)	6
PsbD (c)	D2	39.418 (8)	5
PsbE (c)	α-Cyt *b*559	9.255 (S)	1
PsbF (c)	β-Cyt *b*559	4.409 (S)	1
PsbG	open (not in PSII)	7.697 (S)	
PsbH (c)	H protein	4.195 (S)	1
PsbI (c)	I protein	4.116 (P)	1
PsbJ (c)	J protein	4.283 (S)	1
PsbK (c)	K protein	4.366 (S)	1
PsbL (c)	L protein	3.755 (P)	1
PsbM (c)	M protein	4.722 (T)	1
PsbN (c)	N protein	26.539 (S)	1
PsbO (n)	33 kDa O protein	20.210 (S)	0
PsbP (n)	23 kDa P protein	16.523 (S)	0
PsbQ (n)	16 kDa Q protein	10.236 (S)	0
PsbR (n)	R protein	21.705 (S)	0
PsbS (n)	Lhc-like S protein	3.849 (S)	4
PsbT (c)	(ycf8) Tc protein	3.283 (S)	1
PsbT (n)*	5 kDa Tn protein	15.018 (Sy)	0
PsbU**	U protein	15.121 (Sy)	0
PsbV**	Cyt *c*550	5.928 (S)	0
PsbW (n)*	W protein	4.225 (S)	1
PsbX (n)	X protein	6.541 (S)	1
PsbZ (n)	Z protein		1

Table 1. Proteins that constitute the core of PSII. These proteins are products of the *psbA* to *psbX* genes which occur in all types of oxygenic organisms except for those found exclusively in higher plants and algae (*) or cyanobacteria (**). In eukaryotic organisms the *psb* genes are located in either the chloroplast (c) or the nuclear (n) genomes. The molecular masses of the mature PsbA to PsbX proteins, except PsbU, are calculated from the protein sequences reported in the SWISSPROT database using the MacBioSpec (Sciex Corp., Thornhill, Ontario, Canada) for spinach (S), pea (P), tobacco (T) and *Synechococcus elongatus* (Sy). The number of predicted transmembrane helices is based on hydropathy analyses of primary sequence

Taken from website of http://www.bio.ic.ac.uk/research/nield/psIIimages/PSIIsubunits.html (Ref.3)

photosystem to the reaction center. It is also believed that they interact with proteins associated with the site of water oxidation (15). Biochemical and genetic evidence indicates that CP47 and CP43 may help form the binding site for extrinsic proteins to PS II. The structurally analogous D1 and D2 proteins are at the core of PS II and provide binding sites for a number of important redox-active cofactors in PS II. Cytochrome b559 (cyt b559) is a heme protein in which the heme group is ligated by the two histidine residues in α and β subunits. Many different functions have been postulated for this cytochrome and the most favored is its possible protective role against photoinduced damage of the reaction center. Deletion of the genes for any of these intrinsic proteins results in the complete loss of oxygen evolution activity. Additionally many low molecular mass components appear to be associated with PS II, although the functions of these proteins remain obscure (6).

Three extrinsic proteins with molecular masses of 33, 23, and 17 kDa are required for high rates of oxygen evolution. The 33 kDa protein has been termed the manganese-stabilizing protein (MSP) due to its stabilization of the manganese cluster. The 33 kDa protein is much more tightly associated with the intrinsic PS II proteins than are the 23 and 17 kDa proteins. In the absence of the 33 kDa protein, high concentrations of chloride and calcium are required to maintain the integrity of the manganese cluster (7). The 23 and 17 kDa proteins appear to modulate the calcium and chloride requirements for efficient oxygen evolution. Treatment with high concentration NaCl (1-2 M) can almost totally remove the 23 and 17 kDa proteins from PSII and reduced the oxygen evolution activity significantly. Most of the lost activity can be recovered by the addition of moderate concentrations of calcium and

chloride (8, 9). These three extrinsic proteins interact with intrinsic proteins to yield fully functional oxygen evolving complexes.

c. Manganese cluster

The oxygen evolving complex (OEC) of PS II comprises a tetranuclear Mn cluster, a redox-active tyrosine Y_z and the cofactors Ca^{2+} and Cl^-. The Mn cluster acts both as a catalytic site for water oxidation and as a device for the accumulation of oxidizing equivalents from the reaction center. According to the Kok cycle, the oxidation of water is a four-electron transfer process: the electrons are removed from S_0 to S_4 and O_2 is evolved at S_3 to S_4 to S_0 (10). The point in the cycle where water binds is unknown. The S_1 state is a dark stable state. The S_2 and S_3 states are unstable at room temperature, decaying back to the S_1 state in about a minute. The S_4 state is a transition state with a lifetime of about 1 ms, spontaneously decaying to the S_0 state upon oxygen evolution. At least two, probably all four, Mn atoms are actively involved in the OEC (11). However the Mn valence states remain to be resolved. The most recent x-ray crystallography structure of the Mn cluster was at 3.5 Å solution (Figure 4). The electron density of the Mn cluster was found to fit a cubane-like Mn_3CaO_4 with the fourth Mn ion extending from one corner (12). Three of the manganese ions and the calcium ion are located at four corners of the cube, while the oxygen atoms are at the other corners of the cube. The fourth Mn ion is ligated by one of the oxygens of the cube. This corresponds to the "3+1" Mn tetramer model that was proposed based on EPR spectroscopy (2). The Mn ions in the X-ray crystallography structure have only four or five ligands each, which are less than the required six ligands, indicating that water molecules are probably bound to the cluster

in the remaining sites. The distances for Mn-Mn and Mn-Ca are ~2.7 Å and ~3.4 Å respectively, which are typical for di-μ-oxo and oxo bridges respectively (12).

Calcium is the closest metal to the redox-active tyrosine Z (Y_z) and this short distance (5.1 Å) makes direct oxidation of calcium-bound water possible, although the proton ejected from the tyrosine upon radical formation would not be able to leave via a hydrogen-bonding chain formed through the nearby His 190 in this model (13). However it has been known that the manganese cluster and calcium undergo structural changes in the higher S states of the OEC. It is possible that the structural readjustment can provide an exit pathway for the proton. Then this structural model would be in line with the proposed role of tyrosine as a hydrogen atom abstractor from water.

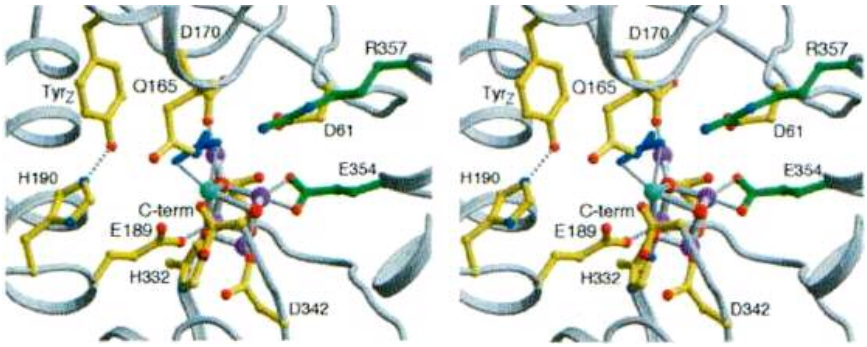

Figure. 4. Stereo view of the OEC with side-chain ligands and possible catalytically important side-chain residues. Mn ions, Ca^{2+}, and oxygen atoms are shown in magenta, cyan, and red respectively. One unidentified nonprotein ligand to the OEC is colored in green (Ref. 12).

Chloride has been suggested to function as a ligand to the manganese cluster, as a bridge between calcium and the Mn cluster, or to compensate for charges accumulated by the manganese cluster during turnover (14). The diversity of chloride effects on PS II may suggest that several different interaction sites or different binding modes exist. Lindberg *et al*. have demonstrated the existence of a pool of slowly exchangeable Cl^- employing radioactive $^{36}Cl^-$ (15). It has been found by

electron paramagnetic resonance (EPR) spectroscopy that the S_2 state modification occurs in the absence of chloride, thereby inhibiting oxygen evolution. The affinity for Cl^- is one order of magnitude lower in the S_2 state than in the S_1 state (16). It has also been suggested that chloride stabilizes the structure of the OEC after removal of the 23 and 17 kDa proteins. A high concentration of chloride is required to maintain the integrity of the Mn cluster when the 33 kDa protein is removed. However questions concerning the number of chloride ions required for function and their locations still remain unanswered.

2. Principle of EPR Spectroscopy

Electron paramagnetic resonance (EPR) spectroscopy can be applied to species having one or more unpaired electrons. Diamagnetic systems are invisible to EPR, since all of their electrons are paired and there is a net spin S = 0 (where S is the highest electron spin quantum number). Commonly encountered paramagnetic species include organic radicals, transition metals and triplet states. The spin of an electron and its associated magnetic moment are the basis of EPR spectroscopy. The electron has two spin states, M_s= +1/2 and M_s = -1/2. In the absence of an applied magnetic field, the two spin states are of equal energy, but split apart in the presence of a magnetic field. The energy of each state is given by:

$$E= g\mu_B B_0 Ms = \pm 1/2\ g\mu_B B_0 \qquad (1\text{-}1)$$

Here is B_0 the strength of the applied magnetic field in Gauss, μ_B is the Bohr magneton, M_s is the electron spin quantum number and g is a proportional factor equal to 2.00232 for a free electron. The value of the g-factor may vary in the range 1.4 to 3.0 for radicals and transition metals. The g-factor is independent of field direction only in isotropic systems or motionally averaged systems which include

dilute liquid solutions of low viscosity and systems with local octahedral symmetry and so on. In anisotropic systems, the value of the g-factor relies on the orientation of the spin system relative to the magnetic field and is described by principal axis values g_x, g_y and g_z. In axial systems, $g_x = g_y = g_\perp$ and $g_z = g_\parallel$. In rhombic systems, the principal g-factors for all three axes are different, $g_x \neq g_y \neq g_z$. The anisotropy of the g-factors is very helpful in understanding the structure surrounding the atom in question.

When an appropriate frequency of radiation is applied to the system, a transition between the two energy levels can occur and be observed by EPR. The frequency (ν) required is directly proportional to the strength of the magnetic field, according to Planck's law:

$$\Delta E = h\nu = g\mu_B B_0 \qquad (1\text{-}2)$$

Usually the frequency is in the microwave region such as 9.5 and 35 GHz for the magnetic fields typically used.

If the electron can interact with a neighboring nuclear magnetic dipole, the two energy levels must be further split (Figure 5) (17), in a process which is called hyperfine coupling. In this case, two transitions can be observed in Figure 5, corresponding to two lines in the EPR spectrum. The energy of each level is given by

$$E = g\mu_B B_0 M_s + a M_s M_I \qquad (1\text{-}3)$$

Here M_I is the nuclear spin quantum number for the neighboring nucleus, and a is the hyperfine coupling constant, which can be obtained by measuring the separation of the two lines in gauss. Theoretically, coupling to a single nucleus of spin n/2 gives (n+1) lines, which have equal intensities (Figure 6) (17); coupling to n equivalent

nuclei of spin ½ again gives (n+1) lines, but the intensities follow the binomial distribution (Figure 7) (17).

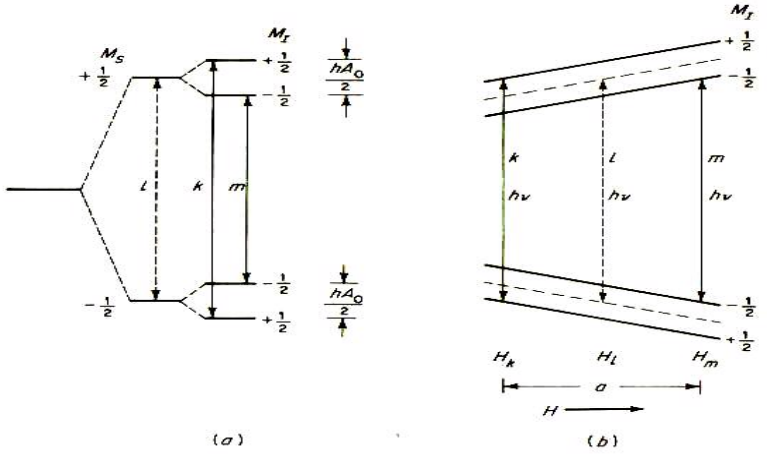

Figure 5. (a) Energy levels of an unpaired electron in a constant magnetic field. The dashed line *l* is the transition in the absence of hyperfine interaction. The solid lines marked *k* and *m* correspond to the transitions with hyperfine coupling. (b) Energy levels of an unpaired electron with variable magnetic field. The dash line *l* corresponds to the transition in the absence of hyperfine interaction. The solid lines *k* and *m* are the transitions with hyperfine coupling induced by the same energy (Ref. 17).

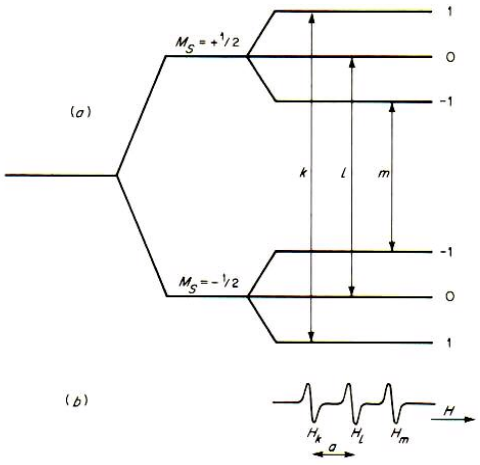

Figure 6. (a) Energy levels and allowed transitions for deuterium atom at constant field. (b) Spectrum at constant frequency (Ref. 17).

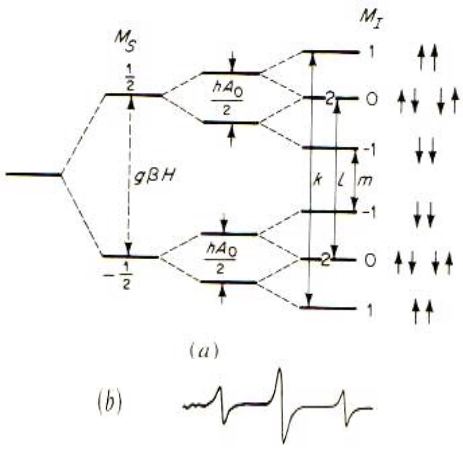

Figure 7. (a) Energy levels and transitions at constant field for two equivalent nuclei with I = ½. Transition *l* is twice as intense as transition *k* or *m*, due to the fact that the l transition occurs between doubly degenerate energy levels. (b) Spectrum at constant frequency (Ref. 17).

Figure 6 shows the energy levels and allowed transitions for the deuterium atom which is a system with S = 1/2 and I =1. The selection rule for an electron spin transition is $\Delta M_s = \pm 1$. If $\Delta M_s = + 1$ when a photon is absorbed, then M_I must remain unchanged to conserve the total angular momentum. Thus the selection rules are $\Delta M_s = \pm 1$ and $\Delta M_I = 0$. These selection rules break down due to the mixing of states when the resonant magnetic field approaches zero.

For a system of an electron interacting with two equivalent protons, it is possible to obtain the appropriate hyperfine energy levels by replacing the two nuclei with one nucleus having I = 1. Figure 7 shows the energy levels and transitions for a system with two equivalent nuclei of I =1/2. Interaction with the first nucleus causes the $M_s = + 1/2$ and $M_s = -1/2$ levels to split; interaction with the second nucleus causes each level to be split again by the same amount of energy. The equivalence implies identity of the hyperfine coupling constants. Twofold degeneracy occurs at the $M_I = 0$ level, which means the population in the $M_I = 0$ states is twice that of the $M_I = +1$ or -1 states. This is reflected in the 1:2:1 relative intensities in the EPR spectrum. For three or more equivalent nuclei with I = 1/2, the repetitive splitting due to each nucleus leads to four or more levels for both $M_s = + 1/2$ and $M_s = -1/2$ states. The intensities of the transitions between these energy levels follow the binomial distribution.

Therefore, the complexity of the EPR spectrum depends on the number and types of the magnetic neighbors of the electron. Without hyperfine coupling, the information provided by EPR spectroscopy would be very limited. The interaction between electron and magnetic nuclei in a complicated system will provide us with a

large amount of information, although computer simulation maybe necessary to interpret the data.

Basic instrumentation of EPR

A typical EPR spectrometer consists of a source of radiation (usually a Gunn diode), a stable magnetic field, a cavity for sample placement, and a detection and recorder system. The Gunn diode emits monochromatic microwave radiation in a small range of frequency. The size of the resonant cavity is chosen so that a standing wave is set up at the source frequency, and the sample is placed in the region of highest energy density. At a fixed microwave frequency, the EPR spectrometer scans a spectrum by a linear variation of the magnetic field. Absorption or emission will occur when the separation of two energy levels is equal to the quantum energy hν of the incident microwave photons.

In principle, the higher the frequency of the radiation source, the higher the sensitivity. But at very high frequency, the sample volume has to be very small to fit within the standing wave and a high magnetic field is also required. Due to these limitations, 9.5 or 35 GHz, corresponding to X-band or Q-band, are the choice for commercial spectrometers.

The heart of the EPR spectrometer is the resonant cavity containing the sample. One half of a radiation wavelength corresponds to the cavity dimension so that a standing wave can be achieved. The wavelength increases with increasing dimension of the cavity. The dimensions of the cavity are typically on the order of about a centimeter for typical frequencies used. The energy density that is associated with traveling microwave radiation is small. However, the energy density produced

by resonance is considerably large and can be stored in the standing waves of the resonant cavity. The standing wave pattern or mode determines the relative position of maximum electric and magnetic fields. The sample is placed in the location where the magnetic field is at a maximum.

The most commonly used detector is a silicon crystal which acts as a microwave rectifier. It converts the microwave power into an electrical current. At incident power level higher than 1 milliwatt, the detector current is proportional to the square root of the microwave power and the detector is called a linear detector. For quantitative signal intensity measurement, the detector should operate in the linear region. For the detector used in most commercial instruments, the best results are attained with a detector current of about 200 microampere. To improve the signal-to-noise ratio, a small-amplitude magnetic field modulation is utilized; therefore the EPR spectrum is usually recorded as a first derivative of the absorption curve (Figure 8).

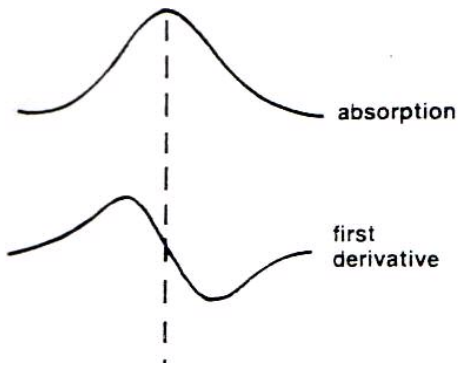

Figure 8. Shapes of absorption and first derivative signals

3. EPR Spectroscopy of Photosyntem II

Photosystem II comprises many electron carriers that can produce diverse EPR signals. The sequence of carriers by which electrons are passed from water to Q_B is shown in Scheme 1 (18). EPR signals have been identified from all of the carriers shown.

Most of the photosynthetic electron carriers give rise to a signal either in the dark-adapted state or after illumination. The paramagnetic states of most species in PS II are generated upon illumination. A short saturating flash of light will cause a single charge separation in every PS II center at 273 K. A reduced electron acceptor and an oxidized electron donor are the products of each stabilized charge separation (Scheme 1). These can be trapped by rapidly cooling an illuminated sample to 77 K, if the sample does not contain compounds that are able to react with the charged species. However some short-lived species may decay during the time necessary to cool a sample or may not be stable even at 77 K. In this case, intense continuous illumination or time-resolved detection methods may be required.

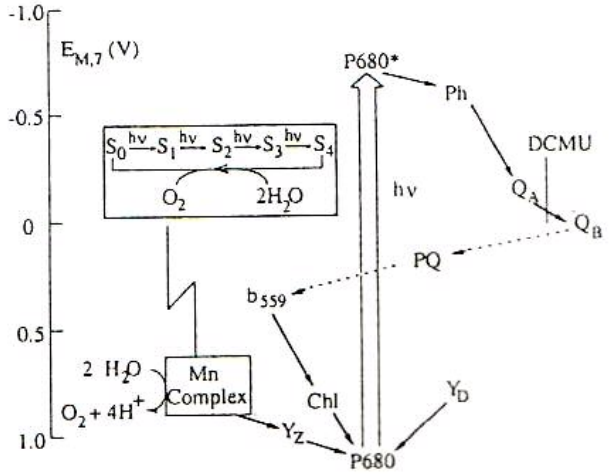

Scheme I. Electron transport among components of Photosystem II. Inset: the Mn complex cycles trough five oxidation states in the course of accumulating oxidizing energy to split water and release oxygen (18).

Tyrosine $Y_D^{\cdot}$

$Y_D^{\cdot}$ can be generated in every PS II center by illumination at 273 K for a minute, and trapped by cooling to 77 K. The $Y_D^{\cdot}$ EPR signal has a g-value of 2.0046, a linewidth of 1.9 mT, and partially resolved hyperfine peaks approximately 0.5 mT apart. The 1:3:3:1 ratio of the lines of the $Y_D^{\cdot}$ signal can be explained by hyperfine coupling of the unpaired electron to two ring protons and one methylene proton. The $Y_D^{\cdot}$ signal is also called signal II_{slow} because it decays slowly in the dark. During oxygen evolution, electron donation from Y_D is much slower than electron donation by water, therefore the latter dominates.

Tyrosine $Y_z^{\cdot}$

Y_z is located on the D1 protein and links the one electron photochemical reaction and water oxidation process. It donates one electron to $P680^+$, forming the $Y_z^{\cdot}$ radical. Because of the short life time of $Y_z^{\cdot}$, the EPR signal from $Y_z^{\cdot}$ is called II_f or II_{vf} (fast or very fast), which decay on millisecond and microsecond timescales respectively, depending on the PSII treatment. The EPR signal of $Y_z^{\cdot}$ has the same lineshape as that of $Y_D^{\cdot}$.

The semiquinone (Q_A^-) and semiquinone-iron complex ($Fe^{2+}Q_A^-$)

Quinone A (Q_A) normally accepts one electron and passes it to quinone B (Q_B) in the electron transport chain. By the time the electron reaches Q_A, the physical separation of the reduced product and the oxidized product is great enough to decrease the possibility of recombination between the two. If illumination is performed at temperatures below 230 K, electron transport from Q_A to Q_B is very slow, and the negative charge can be trapped on Q_A by rapid cooling. Alternatively, DCMU (3-(3,4-dichlorophenyl)-1,1-dimethylurea) can be used to inhibit electron

transport beyond Q_A. The EPR signal of Q_A^- has a g-value of 2.0044± 0.0003 with a linewidth of 0.9 mT in the absence of the iron ion. In the presence of the Fe^{2+} ion, Q_A^- can interact with the nearby Fe^{2+} to produce a 40 mT wide signal at g = 1.9 and 1.64, or a narrower signal at g = 1.82 and 1.67. These two signals represent different forms of the Fe^{2+} Q_A^- pair corresponding to higher and lower pH respectively.

Cytochrome b559

The function of cytochrome b599 remains unclear, although it is indispensable for PSII. Different potential forms of cytochrome b599 are known: high potential, intermediate potential, and low potential forms. The different redox forms are characterized by small changes in the heme coordination (The heme group is ligated by two histidine residues, which are located in the α and β subunits of cytochrome b599, respectively). The EPR spectrum of oxidized cytochrome b559 is anisotropic with g_z ~ 3.00, g_y ~ 2.20 and g_x ~ 1.50, with small variations in these values corresponding to the potential. Direct electron donation from cytochrome b_{559} to $P680^+$ bypassing the physiological donor, the Mn-cluster, is observed only under prolonged illumination at 77 K (19, 20). It has recently been shown that electron donation from the cytochrome occurs via a redox-active carotene (21) rather than via a redox-active chlorophyll as previously thought.

The S_2 state of the Mn complex: the multiline signal and the g = 4.1 signal

The S_2 state EPR signals, including a multiline signal centered at g = 2.0 and a broad signal centered at g = 4.1, were the earliest characterized S-state signals (Figure 9) (22, 23). The g-values and overall widths of the signals, as well as the number of hyperfine lines of the multiline signal, are indicative of a mixed-valence cluster of Mn ions. The discovery of the S_2 state EPR signals provided very useful information for

modeling the structure of the oxygen evolving complex. The signals can be trapped by cooling a sample of PSII to 77 K immediately after illumination in the presence of DCMU or by illumination for several minutes at temperatures below 200 K. Illumination at 160 K and above (in the presence of DCMU) produces constant amounts of the multiline signal. Illumination between 160 K and 120 K results in lower amount of the multiline signal and compensating higher amounts of the g = 4.1 signal with decreasing illumination temperature. The two signals are not from the same spin center, but rather from two different forms of the Mn cluster. The examination of the molecular origin of the two distinct S_2 state signals indicated that a trinuclear and probably a tetranuclear Mn cluster exists in the oxygen evolving complex. The multiline signal, known to arise

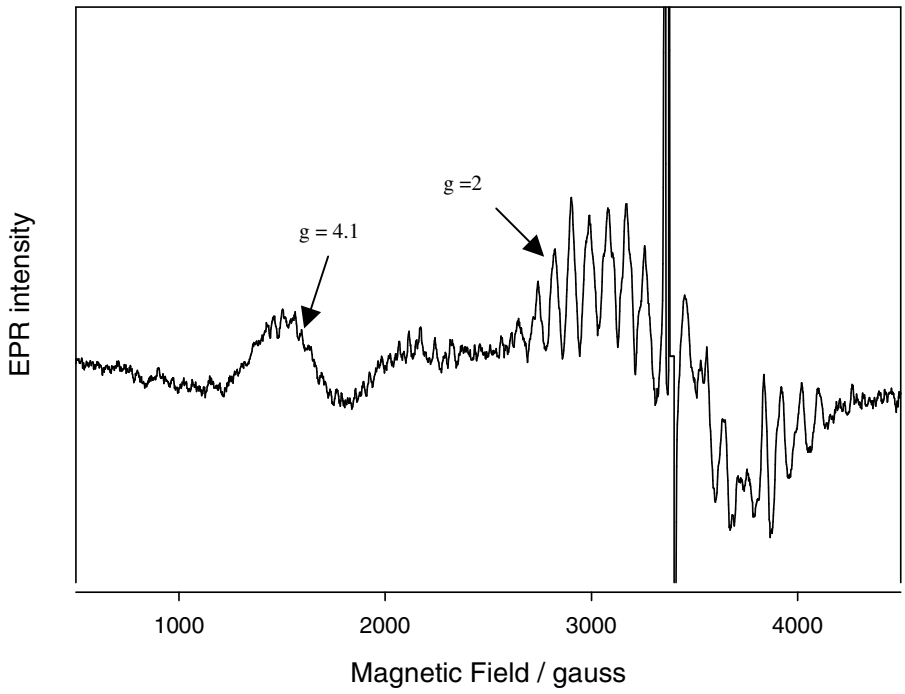

Figure 9. EPR signals arising from the S_2 state of the OEC. The spectrum shown is a difference spectrum of the sample illuminated 8 min at 200 K minus the dark-adapted sample.

from an S = 1/2 state, shows that at least two Mn ions are present in the OEC. For the unique orientation where the membrane was oriented parallel to the magnetic field, the g = 4.1 signal was itself shown to have 'multiline' character in ammonia treated PSII, with at least 16 Mn hyperfine lines present. This showed that the g = 4.1 signal also arises from a multinuclear Mn cluster (22). The ground state of an antiferromagnetically-coupled dinuclear Mn cluster can't give a signal in the g = 4 region (2). Thus at least three Mn ions must be present in OEC. The g = 4.1 signal was further assigned to an S = 5/2 state by Haddy *et al* (23, 24) ruling out the possibility that a single Mn^{IV} ion produced the signal. The tetranuclear Mn cluster model is highly favored because of the possibilities for coupling and has been reinforced by EPR spectral simulations of the multiline signal (25, 26, 27). The latest OEC structural model resolved by X-ray crystallography has shown a distorted cubic Mn cluster with three Mn ions at the corners of the cube and the fourth extending from one corner, confirming the presence of four Mn ions (12).

It has been long reported that calcium depletion affects the magnetic properties of the Mn cluster. The normal multiline signal is lost in Ca^{2+}- depleted PSII and is replaced by another type of multiline signal, which has partially resolved Mn hyperfine lines (A = 5.5 mT, compare the normal A ≈ 8 mT) (28). Substitution of Sr^{2+} for Ca^{2+} also shows an altered form of the S_2 multiline signal with smaller than normal hyperfine splitting (A = 7 mT) and a stabilization of the g = 4.1 signal (29). The recent crystal structure shows the close association of the Ca^{2+} ion with the cubic Mn cluster: Ca^{2+} is on one corner of the cube and connected with Mn by three-μ-oxo bridges. According to the coordination geometry of Ca^{2+}, it is very likely that a water molecule or hydroxide binds to Ca^{2+} at some stage (12).

The effects of chloride on the S_2 state EPR signals have been investigated extensively. Generally chloride is required for the formation of the multiline signal. The removal of chloride induces a shift in the relative intensities of the S_2 state signals toward the g = 4.1 signal. The distribution of the S_2 state signals is restored after chloride is added back (30, 31, 32, 33, 34). The addition of other halide ions such as Br^- and I^- to chloride depleted PS II samples can partially restore the S_2 state multiline signal. Competitive inhibition by F^- causes a loss of the multiline signal with a concomitant increase in the g = 4.1 signal (35, 36).

S_2' state of Mn cluster

Recently, low field EPR signals using both perpendicular and parallel mode detection were observed from the S_3 state. Interestingly the S_3 state was sensitive to near infrared (NIR) illumination. NIR-light excitation of the S_3 state produced a derivative-shaped EPR signal at g = 4.7. It was also found that the S_3 state produced the same signal after long-term incubation at 77 K. This g = 4.7 signal was correlated with the decay of the S_3-state signals and assigned to an S = 7/2 configuration of the S_2 state (denoted S_2') (37). This reported S_2' state signal is of interest because it has not been investigated regarding the effects of chloride and other ions.

CHAPTER II

OVERVIEW OF EXPERIMENTS

The overall goals of the experiments performed here were to determine the Cl^- content in PSII and to examine the anion (Cl^-/ I^-) effects on the S_2' state.

1. Chloride Determination

The chloride requirement in oxygen evolution can be partially satisfied by other anions such as Br^-, I^- and NO_3^-. Previous data showed that a fair amount of oxygen evolution activity was retained after Cl^- depletion (30-40%) (30). Determination of the Cl^- content in the buffers and in PSII is crucial to assessing whether the residual activity is due to a small amount of bound Cl^- after depletion. A previous study employing radioactive ^{36}Cl concluded that about one tightly bound Cl^- was present in each PSII and the dissociation constant of Cl^- in intact PSII was 20 μM (15). So far there has been no Cl^- measurement done on a routine basis in PSII samples. Therefore, the following several experiments were done for this research:

1. *Chloride determination by AgCl colloid assay*

a. The untreated and Cl^- depleted PSII samples were wet-ashed with concentrated HNO_3, then the Cl^- content was assayed by the AgCl colloid assay.

b. The bound Cl^- in PSII was released by Na_2SO_4 treatment at pH 7.5, then the Cl^- content in solution was assayed by the AgCl colloid assay.

2. Chloride determination by Cl^- sensitive microelectrode

The Cl^- content in untreated PSII was directly measured by a Cl^- sensitive microelectrode.

3. Chloride dissociation constant (K_d) determination in NaCl-washed PSII

Known concentrations of Cl^- were added to NaCl-washed PSII samples, and the concentrations of free Cl^- were determined by Cl^- sensitive microelectrode. A Scatchard plot was employed to obtain the K_d for Cl^- binding.

2. Anion Effects on the S_2' State

Chloride has been known to be required for the formation of the multiline signal of the S_2 state and for the S_2-S_3 and S_3-S_0 transitions (38, 39). The S_2' state, an intermediate state between the S_2 and S_3 states, can be produced from the S_3 state by NIR illumination or long term incubation at 77 K. Cl^- may also be required for the formation of the S_2' state since it appears as a result of decay of the S_3 state. Addition of other ions (Br^-, I^-, NO_3^-) to Cl^- depleted PSII can restore the S_2 state partially. If Cl^- is required for the S_2' state, it is very possible that the S_2' state also shows an anion effect.

1. Time dependence of S_2' signal formation

It has been reported that the S_2' signal accumulated during the decay of the S_3 state at 77 K over a period of a week or two (40). A time dependence experiment was done to determine the optimal incubation time, when the S_2' signal was maximally developed. It was expected that the S_2' signal would increase at first during incubation, and then decrease after reaching a maximum. This was done in both intact and Cl^- depleted PS II.

2. *Chloride effect on the S_2' signal*

After the optimal incubation time was found, the examination of the S_2' signal was carried out in the presence and absence of chloride. Both Cl^- depleted PSII and PSII without the 17 and 23 kDa subunits were examined for the effect of Cl^-.

3. *Iodide effect on the S_2' signal*

Iodide activates the OEC in the absence of Cl^-, but is an inhibitor at all concentrations in the presence of Cl^-. It was found in a previous study that the inhibition by I^- occurred at a higher state than S_2 (52). The effect of iodide on the S_2' signal was carried out using following samples:

a. Cl^- depleted PS II with both Cl^- and I^- added. In this case, I^- is an inhibitor.
b. Cl^- depleted PS II with only a small amount (2 mM) of I^-. Here I^- is an activator.
c. Cl^- depleted PS II with an inhibitory amount (25 mM) of I^-.

CHAPTER III

MATERIALS AND METHODS

1. Reagents

Unless otherwise stated, all chemicals were obtained from Fisher Scientific (Fair Lawn, NJ). Potassium ferricyanide and bovine serum albumin (BSA) were obtained from Sigma (St. Louis, MO). Atrazine was obtained from Supelco (Bellefonte, PA). Phenyl-*p*-benzoquinone which was obtained from Aldrich (Milwaukee, WI), was purified by recrystallization from ethanol. The water used in the present experiments was filtered using a Barnstead Nanopure Diamond Lab Water System.

2. General Methods for PSII

a. Intact PS II preparation

PS II-enriched thylakoid membranes were prepared from fresh market spinach as in (42) with little modification. The spinach was first homogenized in Buffer I containing 350 mM sucrose, 20 mM 2-(4-morpholino)-ethanesulfonic acid (MES) and 10 mM NaCl at pH 6.3. Then the sample was centrifuged for 5 minutes at 4400 x g and resuspended to 2.5 mg chlorophyll/ml (mgChl/ml) in Buffer II (20 mM MES, 5 mM$MgCl_2 \cdot 6H_2O$ and 15 mM NaCl at pH 6.3). Then 1/4 volume of 25% Triton X-100 in Buffer II was added to the sample in the dark and incubated on ice for 30 mins to extract PS II-enriched membranes. Finally the extracted membranes were washed in Buffer IV (400 mM sucrose, 20 mM MES, 15 mM NaCl, pH 6.3) three times, each

for 20 mins. The washed membranes were suspended in Buffer IV and stored in liquid nitrogen.

b. NaCl-washed PS II preparation

Intact PS II-enriched membranes were thawed from liquid nitrogen at room temperature and resuspended in buffer containing 2 M NaCl, 0.4 M sucrose and 20 mM MES at pH 6.3 to a concentration of ~0.5 mgChl/ml. The sample was incubated on ice in the dark for an hour or so. Then the treated sample was washed three times with Cl^- free buffer containing 0.4 M sucrose and 20 mM MES at pH 6.3. The PS II pellet was resuspended in buffer containing 0.4 M sucrose, 40 mM MES, 15 mM NaCl and 10 mM $CaCl_2$ at pH 6.3 to a concentration of ~0.5 mgChl/ml for the ferricyanide treatment. Ferricyanide was added to oxidize the non-heme iron Fe(II) to Fe(III). The NaCl-wash treatment removes essentially all 17 and 23 kDa subunits. PS II without the 17 and 23 kDa subunits probably does not retain Cl^- after washing with chloride free buffer.

c. Cl^--depleted PS II preparation

Chloride depletion of PSII-enriched membranes retaining the 17 and 23 kDa subunits were carried out by dialysis using a buffer containing 20 mM Mes-NaOH, pH 6.3, and 0.40 M sucrose. PS II-enriched membranes were thawed from storage and suspended in the buffer to a concentration of 0.5-0.8 mgChl/ml. The samples were then centrifuged at 13,900 x g for 10 min to pellet. The pellets were resuspended in the same buffer and centrifuged again. This wash step was repeated two more times to remove the non-specifically bound chloride from the samples. The samples were then resuspended to a concentration of ~2.1 mgChl/ml and placed in dialysis tubing of molecular weight cut-off 15 kDa (Spectrum Laboratories, Laguna Hills,

CA). The samples were dialyzed against the Cl^- free buffer at 4 ºC for ~25 hours in the dark. These PS II membrane fragments will be referred to as Cl^--depleted. The estimated chloride concentration after dialysis was 20-40 μM based on measurements by AgCl colloid assay. The Cl^--depleted PSII membranes were then centrifuged and stored in liquid N_2.

d. Oxygen evolution assay

Oxygen evolution assays were carried out using a Clark-type oxygen electrode (model 5331, Yellow Springs Instruments, Yellow Springs, OH). PS II samples were thawed and suspended to the concentration of ~1.0 mgChl/ml in control buffer containing 0.4 M sucrose, 20 mM MES-NaOH, pH 6.3, and 15 mM NaCl. Oxygen concentration was calibrated using air-saturated distilled water and water purged of O_2 using N_2 gas. Samples were exposed to saturating light using a Dolan-Jenner (Lawrence, MA) model 180 Fiber-lite high intensity illuminator and a 500 W projector lamp. OxyGen 3 (written by Sergei Baranov) was the program used to accumulate data and calculate the oxygen evolution rates. The assays were carried out at 25 ºC with 1 mM phenyl-*p*-benzoquinone (PPBQ) as electron acceptor added from a 50 mM stock solution in dimethylsulfaxide. The oxygen evolution rates of PS II samples were measured at least three times and the averages were taken to ensure the accuracy of the measurement.

e. Determination of chlorophyll concentration

Chlorophyll was extracted from PSII by directly adding 80% of acetone. Then the sample was mixed well and centrifuged for 2 min. The absorbance of the supernatant was measured at 645 and 663 nm. The concentration of chlorophyll can be obtained by following equation,

$$C = 20.2\ A_{645} + 8.0\ A_{663} \quad (3\text{-}1)$$

Here C is the concentration of chlorophyll in mg/ml, A_{645} is the sample absorbance at 645 nm, and A_{663} is the absorbance at 663 nm.

3. Cl^- Determination Procedures

a. Wet-ashed PSII assay

The PS II samples (~2.5 mgChl/ml) were wet-ashed overnight at 60ºC using 2 times the volume of concentrated HNO_3. After the thick dark-green samples turned clear yellow, the sample was neutralized with 10 M NaOH and then bleached with 30% H_2O_2.

b. Removal of 17, 23 kDa proteins and Cl^- by sulfate treatment

Intact PS II stored in liquid nitrogen was thawed and suspended in chloride free buffer containing 0.4 M sucrose and 20 mM MES (pH 6.3) in a 1: 30 volume ratio. The samples were centrifuged at 20,000 rpm for 10 min in the JA20 Beckman rotor, and the pellets were washed in the same buffer with the same volume three times, each for 10 min, to remove all non-specifically bound Cl^- ions. The final pellets were then incubated in a buffer containing 50 mM Hepes (pH 7.5), 0.3 M sucrose, and 50 mM Na_2SO_4 at a Chl concentration of 0.2 mg/ml in the dark for 30 min. The concentration of PS II in mol/l is estimated to be

$$[Chl]/\ mg/ml * 1/\ (900\ g/mol) * 1/200 \quad (3\text{-}2)$$

The molecular weight of chlorophyll in PSII is about 900 g/mol, and each PSII is estimated to contain 200 chlorophylls.

The samples were then centrifuged at 20,000 rpm for 10 min. The supernatant containing the 17 and 23 kDa proteins and chloride were saved for the determination of the concentration of chloride.

c. AgCl colloid assay

The silver nitrate was added to the sample in order to determine the concentration of chloride (15). A calibration curve was made using known concentrations of Cl^- (0-60 µM) in the same buffer added as NaCl. The absorbance was measured at 400 nm 30 min after the addition of 2 mM $AgNO_3$. At low concentrations of Cl^-, no clearly visible precipitate of AgCl was formed, but when exposed to room light for 30 min, the solutions darkened due to photochemically-formed colloidal silver in proportion to the amount of AgCl present.

d. Cl^--sensitive electrode assay

A Cl^- sensitive microelectrode (Lazar Research Laboratories, Los Angeles, CA) was connected with an Accumet AR50 pH/mV/Ion/Conductivity meter (Fisher Scientific). The AR50 meter was set to ion mode. The benefit of using a microelectrode is that the sample size can be as small as 5 µl and the microelectrode can be immersed only 1 mm below the sample surface to allow contact between the solution and the electrode sensing element. The potential in millivolts detected by the meter is proportional to the log of Cl^- concentration. Given ideal conditions, the lowest concentration that can be detected is about 10 µM. In the present experiments, the calibration curve was prepared between 0.05 and 200 mM.

e. Determination of dissociation constant for chloride

For the study of chloride dissociation, intact PS II was thawed and treated with 2 M NaCl to remove the 17 and 23 kDa subunits as indicated. Then the samples were

washed three times by centrifugation in Cl^- free buffer containing 0.4 M sucrose and 20 mM MES (pH 6.3) to remove the chloride. The final pellets were resuspended to a concentration of ~3 mgChl/ml. The PSII sample was titrated with NaCl, with a total change of volume of less than 10%. After each NaCl addition, the free chloride concentration was measured using a Cl^- sensitive microelectrode (Lazar, Los Angeles, CA). Each data point was read 1 min after Cl^- was added at 4°C.

If PSII has a single binding site for Cl^-, then for the dissociation of Cl^- from PSII is given by

$$PS\text{-}Cl \rightarrow PSII + Cl^-$$

The dissociation constant (K_d) for chloride is

$$K_d = \frac{[PSII]\,[Cl^-]}{[PSCl]} \tag{3-3}$$

The total PS II concentration, $[PSII]_{tot,}$ equals $[PSII]$ plus $[PSCl]$, so

$$[PSII] = [PSII]_{tot} - [PSCl] \tag{3-4}$$

Substituting equation (3-3) into (3-2)

$$K_d = \frac{([PSII]_{tot} - [PSCl])\,[Cl^-]}{[PSCl]} \tag{3-5}$$

Equation (3-4) can be rearranged to

$$\frac{[PSCl]}{[Cl^-]\,[PSII]_{tot}} = \frac{1}{K_d} - \frac{[PSCl]}{K_d\,[PSII]_{tot}} \tag{3-6}$$

From equation (3-5), a plot of $[PSCl]/[Cl^-][PSII]_{tot}$ versus $[PSCl]/[PSII]_{tot}$ yields a line with a slope of $1/K_d$ from which K_d can be determined. This plot is called a Scatchard plot (43).

If the enzyme has multiple binding sites and these sites are counted independently, even though they may be on the same PSII molecule, the number of binding sites can also be determined by Scatchard plot. In this case, the total concentration of free Cl^- sites is given by,

$$[PSII] = n\,[PSII]_{tot} - [PSCl\,]$$

where n is the number of the binding sites for Cl^- per PSII and PSCl represents a bound Cl^-. Thus the dissociation constant (K_d) for chloride is

$$K_d = \frac{[PSII]\,[Cl^-]}{[PSCl]} = \frac{(n[PSII]_{tot} - [PSCl])\,[Cl^-]}{[PSCl]} \qquad (3\text{-}7)$$

In the same way, we obtain

$$\frac{[PSCl]}{[Cl^-]\,[PSII]_{tot}} = \frac{n}{K_d} - \frac{[PSCl]}{K_d\,[PSII]_{tot}} \qquad (3\text{-}8)$$

If $[PSCl]/([Cl^-][PSII]_{tot}$ is plotted versus $[PSCl]/[PSII]_{tot}$, the intercept of the x axis is n.

4. EPR Spectroscopy

a. Addition of Cl^- and I^- to the Cl^- depleted PSII

The Cl^--depleted PSII membranes were thawed at room temperature and resuspended to a concentration of ~0.5 mgChl/ml. The sample was split into four parts. Then they were treated with 15 mM NaCl, 2 mM NaI, 25 mM NaI and 15 mM NaCl / 50 mM NaI, respectively. Then they were incubated on ice in the dark for ~30 min. Then the samples were ready for ferricyanide treatment.

b. Ferricyanide treatment

The ferricyanide treatment was carried out as in (37) with little modification to oxidize the acceptor side iron, a prerequisite for S_3 state production. The PS II-enriched membrane fragments were treated with 2 mM ferricyanide added from a 20 mM stock solution and incubated on ice in the dark for 30 min to oxidize the acceptor-side nonheme iron. The oxidant was subsequently removed by 3-4 wash steps with corresponding ferricyanide-free buffer by centrifugation at 35,000 × g. The final pellet was resuspended in ferricyanide-free buffer supplemented with 0.2 mM atrazine to a concentration of 5-6 mgChl/ml. After incubating on ice in the dark for ~1 hour, the samples were transferred to EPR tubes.

c. Preparation of EPR samples

EPR samples were prepared in 4-mm outer diameter clear fused quartz tubes (Wilmad Glass) at a concentration of 5-6 mgChl/ml or more. The samples were loaded into the tubes using a 1cc syringe (Becton Dickinson & Company) with a length of very thin intramedic tubing connected to the needle. The sample height was about 3 cm. Samples were then dark adapted on ice for ~1 hour, frozen, and stored in liquid nitrogen.

d. EPR spectroscopy

EPR spectroscopy was carried out at 9.5 GHz with a Bnker Instruments EMX EPR Spectrometer (Billerica, MA). The spectrometer was equipped with a standard ER4102ST cavity and the operating temperature was controlled by an Oxford Instruments (Eynsham, UK) ESR 900 liquid helium cryostat. The spectra were recorded at 10 K. The EPR settings were microwave power of 20 mW, modulation frequency of 100 kHz, and modulation amplitude of 20 G. Frequency was monitored

using an EMX 048T frequency meter. Either six or four scans from 500 to 4500 G or from 0 to 5000 G were averaged for each spectrum. The spectra of dark-adapted EPR samples (S_1 states) stored in liquid nitrogen were first recorded. Then the EPR samples were rapidly transferred into a 195 K precooled ethanol bath for illumination. Two Dolan-Jenner 180 Fiber-lite high intensity illuminators were used for the illumination. To avoid warming up the samples, the light was filtered through a solution of 5 mM $CuSO_4$. The samples were advanced to the S_2 state using 8 min illumination, and then the spectra were recorded. Advancement to the S_3 state was achieved by illuminating the EPR samples for 8 min at 240 K (44). This procedure yielded about 50-60% S_3 and 50-40% S_2 state (37). PSII centers that did not have oxidized iron and S_3 state PSII centers that were reduced by the Y_D radical during the illumination were considered to account for the main contribution to the S_2 state (37). The S_2' state was produced by incubating the S_3 state PS II at 77 K for several days. The other way to generate the S_2' state is to illuminate the S_3 state PS II using IR light at 50 K for a total of 3 min with 30 s interval. This method was also tried, although it did not work under present conditions, probably because of insufficient IR intensity of the source.

e. Time dependence of formation of S_2' signal.

EPR samples in the S_3 state were stored in liquid nitrogen to allow decay to the S_2' state. The dependence of the S_2' state formation on the time of incubation was determined by recording the spectra of the same sample every 2-3 days for a total of 29 days. The height of the S_2' state signals were measured to find the optimum incubation time.

CHAPTER IV

RESULTS AND DISCUSSION: CHLORIDE DETERMINATION

Chloride has been known as an essential cofactor of the OEC and depletion of chloride lowers oxygen evolution activity. EPR and Fourier transform infrared difference spectroscopy (FTIR) show abnormal properties of the Cl^--depleted OEC in the S_2 state, suggesting that chloride is closely associated with the Mn cluster but not as a direct ligand (34, 45). However questions concerning the number of chloride ions required for normal function and their location are still unanswered. An approximate value of about 1 Cl^-/PSII of slowly exchanging Cl^- (time scale of hours) was obtained by measuring the radioactively labeled ^{36}Cl in PS II prepared from spinach grown in radioactive Cl^- (15, 46). Since there was no non-exchangeable chloride in PS II and the radioactivity was not permanently associated with the PS II membranes, the uncertainty involved in setting the zero time point for the release of chloride makes the accurate determination of tightly bound chloride difficult.

The conclusion by the same authors that chloride is not absolutely required for oxygen evolution is based on the experiment in which chloride-depleted PS II still showed oxygen-evolving activity at low levels of 30-40% (30). However whether the depletion of chloride was complete is still questionable since the radioactivity measurement of chloride binding needs to be further confirmed. So, precise determination of the chloride concentration in untreated and chloride-depleted PS II is important for understanding the function of chloride in PS II.

1. Chloride Determination in PSII by AgCl Colloid Assay

a. Cl^- content in wet-ashed PSII samples

We attempted to measure Cl^- in untreated and Cl^- depleted PS II after wet ashing using the AgCl colloid assay. The calibration curve was made in buffer medium that contained all reagents added during sample preparation, but without the sample (Figure 10). At low Cl^- concentrations (<100 μM), the linear relationship between the absorbance and concentration of Cl^- was maintained very well according Beer's law. This assay is a little tricky because formation of the AgCl colloid is photo-sensitive, therefore a consistent exposure time to room light is required to obtain accurate result. Increase in the absorbance of the standard solution containing NaCl after addition of $AgNO_3$ was observed with longer exposure times, and the absorbance reached 93% of the maximum after 30 min exposure under room light (Figure 11). In the present study, all absorbance readings were taken 30 min after the addition of $AgNO_3$ to the buffer medium or samples.

The concentration of Cl^- in PS II samples that had been washed to remove excess Cl^- was expected to be in the micromolar range after the wet-ashing and peroxide treatment of the sample, given one Cl^- per PSII. To measure such trace amounts of chloride, the method of standard additions is more reliable than direct measurement in the presence of interfering species. Known concentrations of Cl^- were added to PS II samples with the expectation that the concentration of Cl^- in the original solution could be found by extrapolation of the absorbance readings to zero addition. However this method did not give a satisfactory result (Figure 12), with the absorbance decreasing with added Cl^- instead of increasing. Since in the absence of the PS II sample, the absorbance obeyed Beer's law, it was thought that the

components from the treatment of PS II interfered with the absorbance, giving anomalous results. During the wet-ashing and bleaching procedure, the PS II membrane proteins were probably broken to small peptides, even single amino acids, and the metal ions and lipids were totally released to the solution. The electrolyte concentration in the solution was apparently so high that coagulation of AgCl colloid, even precipitation, occurred, resulting in the absorbance decreasing with the increase in chloride concentration. This was demonstrated by the increasing dark precipitation at the bottom of the cuvette and decrease in absorbance of the sample as the sample sat in the room light for longer times (Figure 13). Some coagulation of the AgCl colloid also occurred in samples used for the preparation of the calibration curve, but the situation was not as severe as in the samples with PS II.

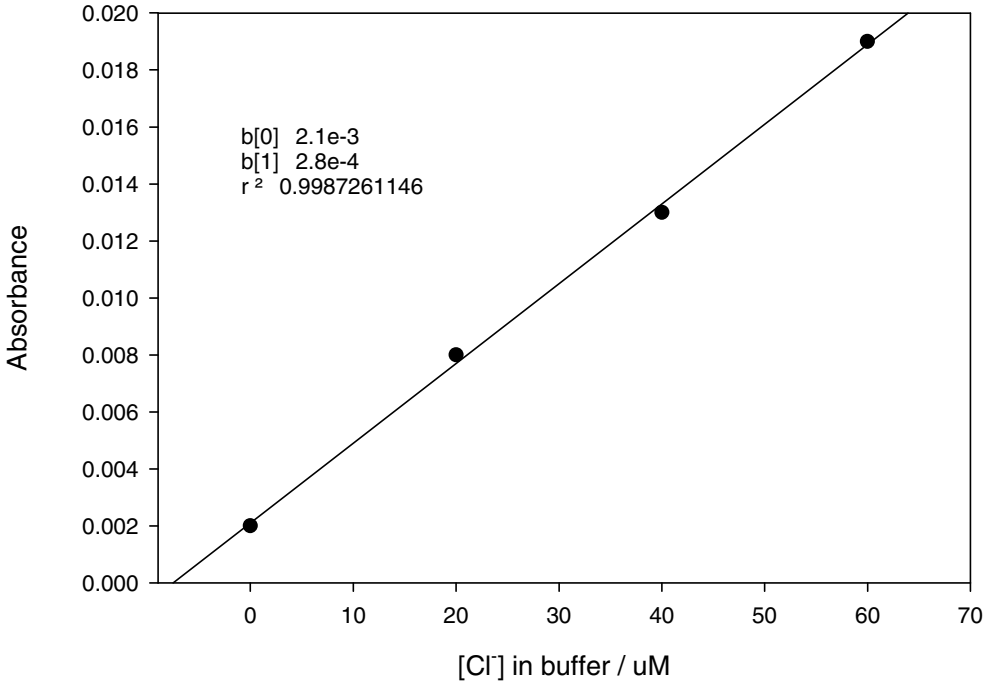

Figure. 10. Calibration curve for the measurement of Cl^- by the AgCl colloid assay

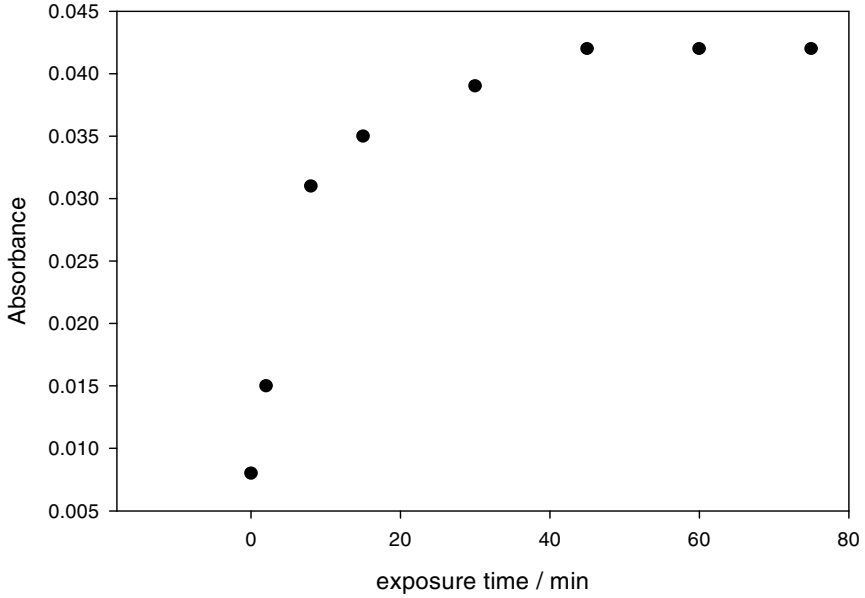

Figure 11. Absorbance increase with exposure time to room light after addition of $AgNO_3$ to buffer containing 30 µM NaCl

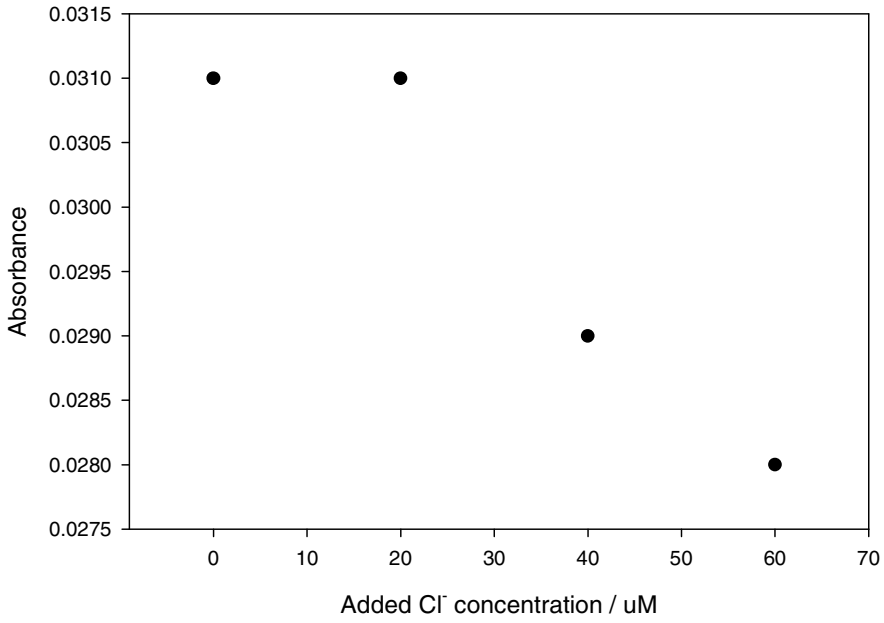

Figure 12. Determination of Cl^- in wet-ashed PS II sample by the standard addition method

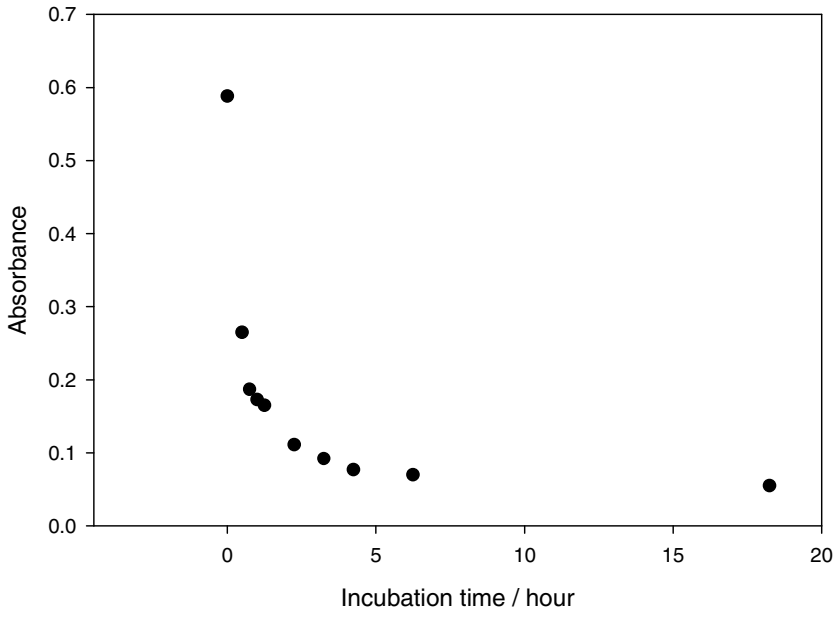

Figure 13. The absorbance of the wet-ashed PSII decreased with the exposure time after $AgNO_3$ addition. No additional Cl^- was added to the sample

Sufficient dilution of the PSII sample could decrease the concentration of electrolyte in the buffer, therefore eliminate the coagulation problem. However the concentration of Cl^- in diluted sample was too low to be detected.

To further elucidate the interference caused by protein, 11 mg/ml of bovine serum albumin (BSA) was wet-ashed in the same way. It was found that wet-ashed BSA produced a high background absorbance. The absorption spectrum was scanned from 200 nm to 800 nm and high absorbance was observed below 400 nm. The reason why wet-ashed BSA produced a higher background than untreated BSA was not clear to us, but at least this experiment indicated that proteins introduce a high background absorbance. It was concluded that in general, the wet-ashing method should be avoided because of the complicated background absorbance, time-

consuming preparation (at least 24 hours for wet-ashing and bleaching), and the additional dilution factor introduced in the bleaching step.

b. Release of Cl⁻ from PSII by incubation at pH 7.5 in the presence of sulfate

To avoid the interference caused by the presence of the PS II-enriched membrane itself, chloride was released from the PS II membrane, and then detected in a relatively simple environment. It has been known that the 17 and 23 kDa extrinsic proteins and presumably chloride can be released by 15 min of incubation in a buffer containing 50 mM Hepes (pH 7.5), 0.3 M sucrose, and 50 mM Na_2SO_4 (38, 47). In this experiment, after extensive washing of the PSII to remove nonspecifically bound Cl^-, as indicated in the Methods section, no detectable chloride was present in the supernatant. Intact PS II membranes were incubated at pH 7.5 in the presence of sulfate, so that chloride was released from the PS II membranes and retained in the supernatant after centrifugation. The concentration of chloride in the supernatant after centrifugation was obtained by extrapolation using the standard addition method (Figure 14). The concentration of contaminating chloride in the buffer medium was obtained in the same way (Figure 15). The concentration of Cl^- in PSII was obtained by subtracting the contaminating Cl^- from the supernatant (Table 2).

Table 2. Cl^- content released from intact PSIIby Na_2SO_4 at pH 7.5

[Chl] mg/ml	[PSII] µM	[AgNO3] mM	[Cl^-] in supernatant µM	[Cl^-] in buffer µM	[Cl^-] in PSII µM	Cl^-/PSII
0.244	1.24	2.00	3.78	2.00	1.78	1.4
0.244	1.24	0.20	2.25	0.73	1.52	1.2

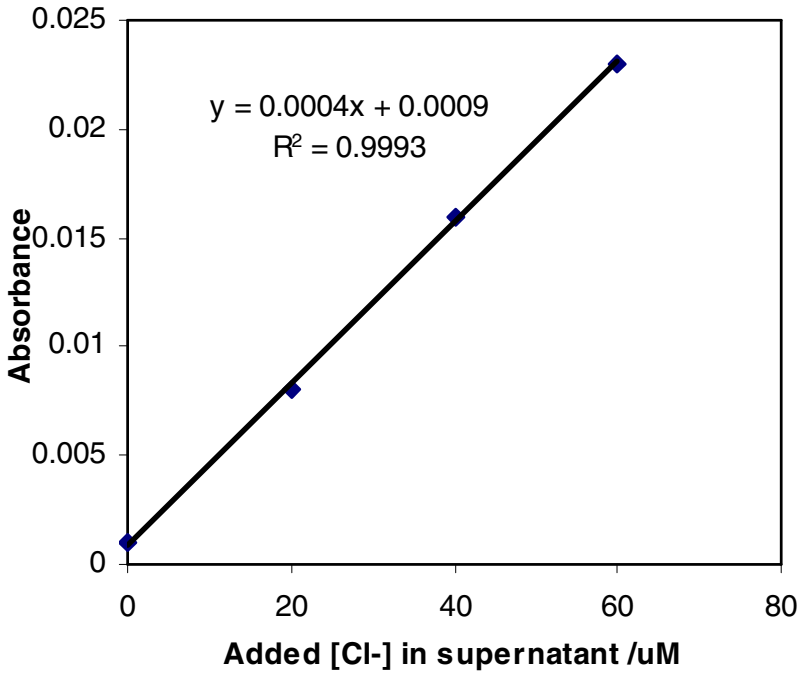

Figure 14. Determination of Cl^- content in the supernatant after centrifugation of PSII by the method of standard additions .

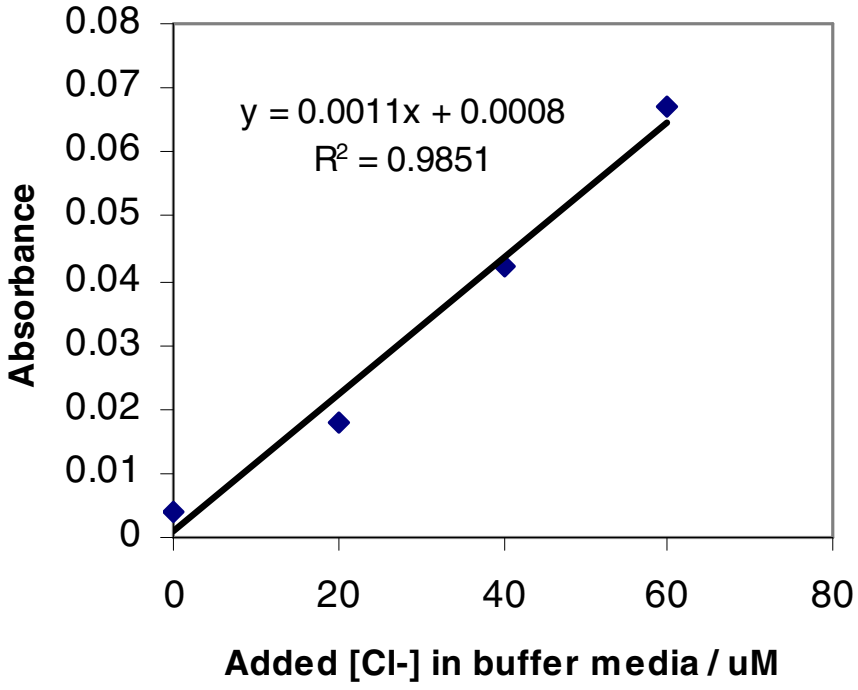

Figure 15. Determination of Cl^- content in the buffer medium by the method of standard addition

It was found that each PSII molecule contained approximately one high affinity Cl^- (1.4 and 1.2 Cl^-/PSII respectively), which was consistent with the result obtained from radioactive measurement (15).

The Cl^- contamination of buffers was routinely found to be in the range 20-40 μM Cl^- (38) which was also found in our lab. However, the chloride contamination could be reduced by carefully rinsing the containers and equipment in the fresh purified water before use, wearing gloves throughout the experiment, and using highly purified reagents. It was found that the chloride contamination in buffer without MES (< 5 μM usually) was much lower than in buffer containing MES (~20 μM). In addition, the chloride contamination could be further reduced by adding a lower amount of $AgNO_3$. Table 2 showed that the contaminating Cl^- in the buffer was lower when the final concentration of $AgNO_3$ was 0.2 mM instead of 2.0 mM. There were no detectable amounts of Cl^- in the Nanopure water used in this experiment. However one can question the accuracy of the result because the concentration of chloride in this experiment was so close to the detection limit of the AgCl colloid assay, which is 1 μM (15). Efforts to concentrate the sample were made by blowing nitrogen over the sample, but the high viscosity caused by the concentrated sucrose in the buffer limited the concentration of the samples. Although further improvement needs to be made, the current method provided a regular, simple measurement of Cl^- released from the PS II membranes, and the result obtained matched that of the previous radioactive ^{36}Cl method (46).

It was thought that the Cl^- concentration in Cl^- depleted PSII samples would be too low to be detected by releasing the Cl^- from PSII to the buffer in the same way as above. It was expected that the Cl^- concentration in Cl^- depleted sample would be

about the same as in the releasing buffer (50 mM Hepes, 0.3 M sucrose, and 50 mM Na_2SO_4, pH 7.5), therefore it could not be detected by the AgCl colloid assay.

2. Chloride Determination in PSII Using a Cl^- Sensitive Microelectrode

Under ideal conditions, the lowest concentration that can be detected using the Cl^- sensitive microelectrode is about 10 μM. In the present experiments, the calibration curve was prepared between 0.05 and 200 mM (Figure 16). At concentrations lower than 0.05 mM, the electrode readings were no longer consistent and the experimental error became very large. In this case, to bring Cl^- into the detectable range, the PSII concentration must be higher than 0.05 mM (corresponding to 9 mgChl/ml), given 1 Cl^-/PSII. However the PSII samples were very thick at such

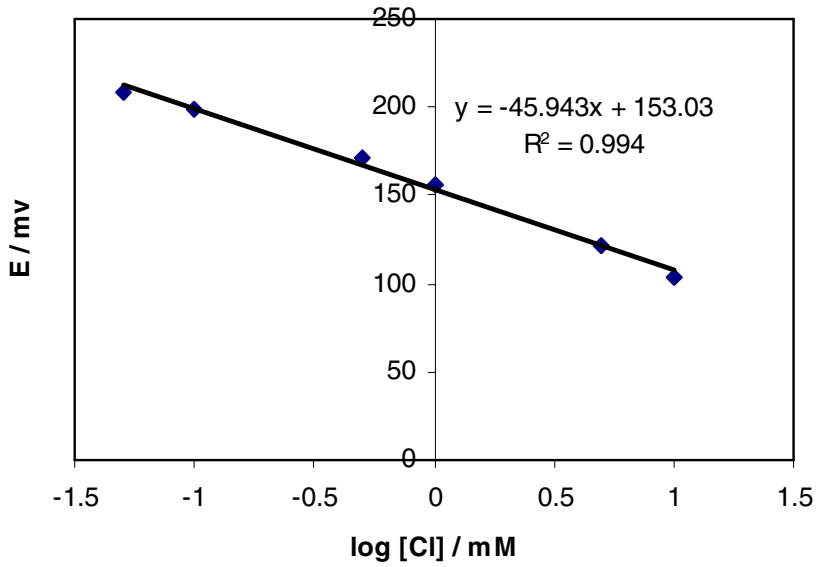

Figure 16. Calibration curve for Cl^- determination by Cl^- sensitive microelectrode

high concentrations, so that the response time of the electrode became longer and the behavior the electrode was not predictable. No reliable data were obtained so far by

direct measurement of Cl^- content in PSII using the Cl^- microelectrode. Other pretreatments such as wet-ashing and Cl^- releasing tended to dilute the sample and make the Cl^- concentration even lower. In summary, the Cl^- electrode was not sensitive enough to detect the chloride in PSII samples directly.

3. Determination of Dissociation Constant for Chloride

In previous experiments (Lindberg *et al.*,1990), PS II membranes isolated from spinach grown on medium containing $Na^{36}Cl$ were found to have a binding site for one Cl^- ion that is in slow exchange with the surrounding medium. This tightly bound Cl^- ion was found to have a dissociation constant of about 20 μM and a dissociation time of 1 hour (15). This result was highly dependent on the integrity of the PS II. Removal of the extrinsic 17 and 23 kDa proteins seems to accompany with the loss of the high affinity, slow exchanging binding site. In a PS II preparation depleted of the extrinsic 17 and 23 kDa proteins by incubation at pH 7.5 in the presence of 50 mM sulfate, a dissociation constant of 6.5 mM for Cl^- was estimated based on O_2 evolution assay (16). The Cl^- binding and equilibrium took place within 10 s and 50 mM Cl^- was saturating in this polypeptide-depleted PSII preparation (16).

In the present experiment, NaCl-washed PSII membranes, which did not contain Ca^{2+}, Cl^-, or extrinsic 17 and 23 kDa proteins, were used to determine the Cl^- affinities. The free chloride in the PSII samples was measured using a chloride sensitive microelectrode as indicated in the Methods section after addition of different amounts of chloride in the form of NaCl. Data in Figure 17 showed that the concentration of bound chloride reached a maximum after addition of 20 mM of NaCl, and then decreased with further addition of NaCl. This unusual behavior

suggests that higher concentrations of NaCl (>25 mM) caused release of bound chloride from the NaCl-washed PSII. When very high concentrations of NaCl (>50 mM) were added, the amount of bound chloride appeared to be negative, indicating that PSII was not capable of binding any chloride that had been added, and even released more chloride that had been bound prior to Cl^- addition.

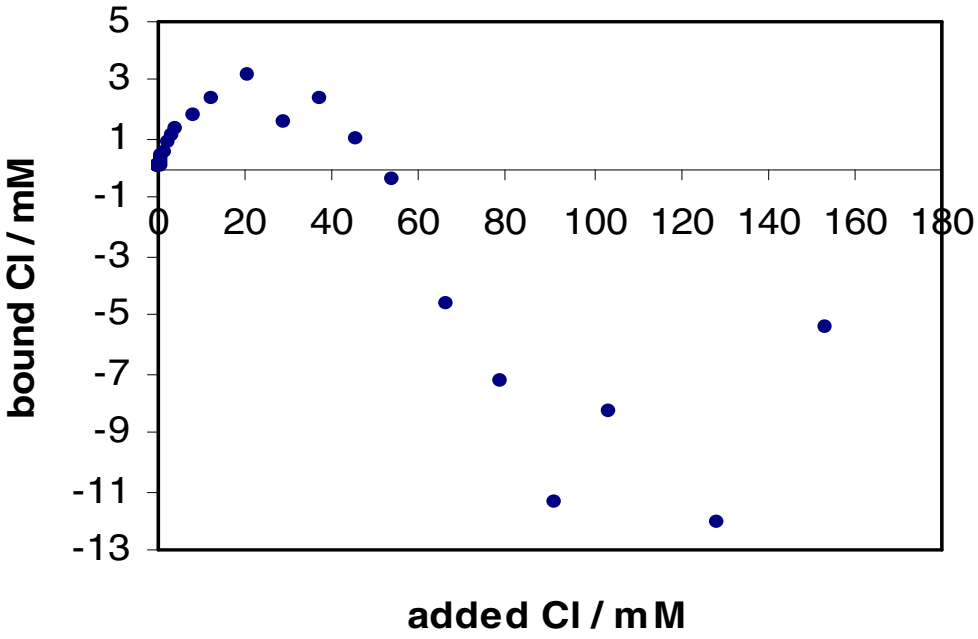

Figure 17. Chloride binding to NaCl-washed PSII. $[PSII]_{tot}$ was 0.02 mM. The bound $[Cl^-]$ in PSII was obtained by subtracting free $[Cl^-]$ from added $[Cl^-]$.

In this experiment Na^+ was added to the samples as the Cl^- counterion. It has been found that in the absence of the 17 and 23 kDa proteins, monovalent cations (Na^+, K^+, Cs^+) inhibit the calcium binding site responsible for activation of the OEC (48, 49). Na^+ displayed a mixed-type of inhibition and the K_i value for Na^+ was estimated to be in the range of 8 mM (49). Na^+ became more inhibitory for oxygen evolution as the concentration increased. NaCl also produced kinetics indicative of

non-competitive inhibition of the Cl^- binding site. This inhibition can be attenuated by increasing the concentration of Ca^{2+}.

Here, the unusual binding results can be interpreted as resulting from Na^+ inhibition. In the absence of Ca^{2+}, as the concentration of Na^+ increased, its non-competitive inhibition for the Cl^- binding site became more pronounced. When the concentration of Na^+ was higher than 20 mM, the inhibitory effects of Na^+ on the Cl^- binding sites dominated the Cl^- binding activity, resulting in the release of bound Cl^- from the PSII sites. Finally all bound Cl^- was released from the PSII with the increase in NaCl concentration. The NaCl-wash treatment was thought to remove all Cl^- from PSII membranes, but in this study it appeared that there was still Cl^- in PSII after NaCl-wash treatment because the amount of free Cl^- in the solution was higher than the amount of added Cl^- after more than 50 mM Cl^- was added. It is not sure whether the extra chloride is from PSII or some unknown factors that affected the measurement of Cl^-.

A Scatchard plot (Figure 18) was made to examine the Cl^- binding affinity by plotting $[PSCl]/([Cl^-][PSII]_{tot}$ versus $[PSCl]/[PSII]_{tot}$ (equation 3-8). When the concentration of added NaCl was higher than 20 mM, the Cl^- started to be released from PSII by a mechanism that is still not quite clear as discussed above. So only the data obtained at Cl^- concentrations lower than 20 mM were used to examine the binding affinity of Cl^- in NaCl-washed PSII. The truncated data of Figure 18 is shown in Figure 19. The Scatchard plot revealed two different classes of binding sites present in the NaCl-washed PSII samples. Data were analyzed to give two dissociation constants with K_{d1}= 53 μM and K_{d2}= 4.2 mM. The numbers of corresponding binding sites were 7 and 170.

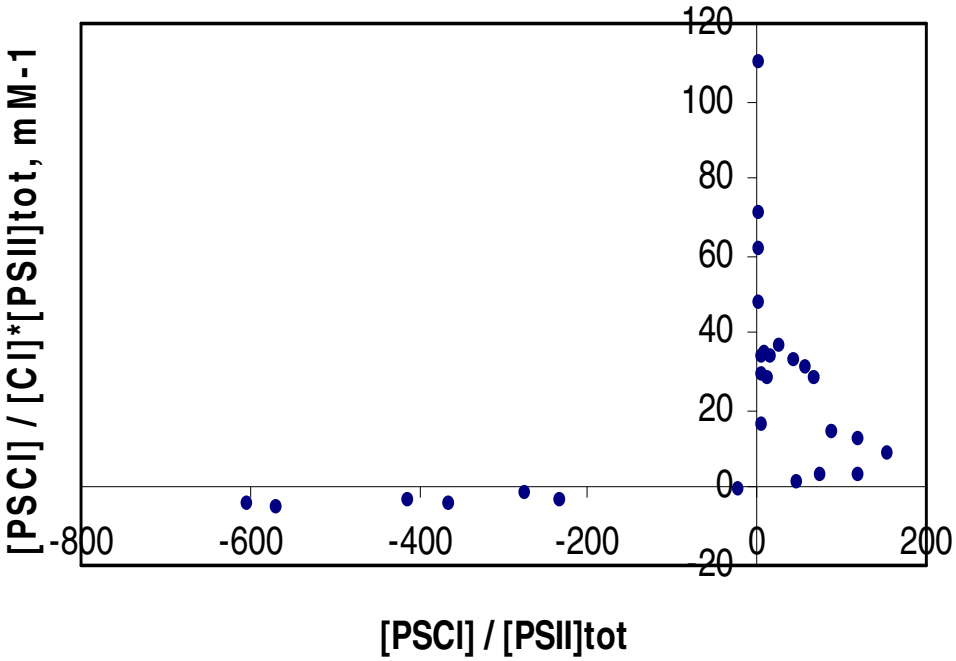

Figure 18. Scatchard plot of Cl^- binding to NaCl-washed PSII. $[PSII]_{tot}$ was 0.02 mM. The [PSCl] was equal to bound $[Cl^-]$, obtained by subtracting free $[Cl^-]$ from added $[Cl^-]$.

The extremely large number of binding sites indicated that chloride binds to PSII non-specifically in the absence of the 17 and 23 kDa proteins. These extrinsic proteins in PSII provide a binding pocket for chloride and act as a barrier at the same time (50) to prevent chloride exchanging with the environment rapidly. The removal of the 17 and 23 kDa proteins removed the chloride exchange barrier, thus chloride can access the OEC more easily. It is suggested that exposure of the protein surface that binds the 17 and 23 kDa proteins also results in pronounced non-specific binding. The K_{d2} (4.2 mM) was comparable with the results obtained in other 17 and 23 kDa polypeptide depleted PSII samples, although the number of sites was not determined in that study (16). The binding associated with K_{d1} (53 μM) may come from the small

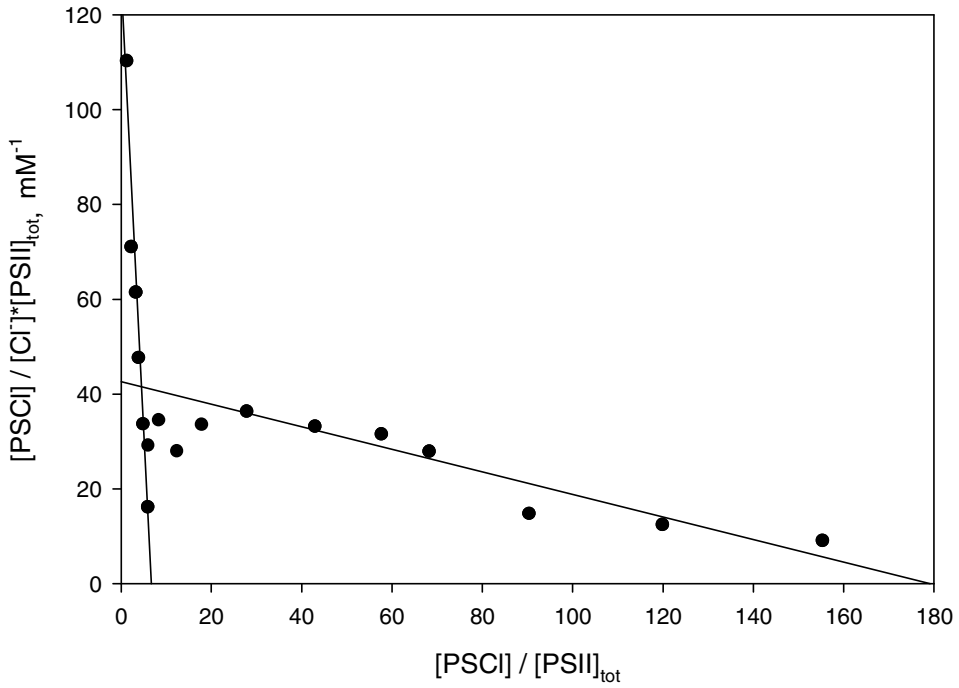

Figure 19. Truncated data from Figure 18, for added [Cl^-] less than 20 mM.

fraction of PSII in which the 17 and 23 kDa proteins were not removed by the NaCl-wash step. It was found the NaCl-washed PSII still retains 5-10 % of the 23 kDa protein (48). The value of K_{d1} was just 2-fold higher than the value obtained in radioactive labeled intact PSII membranes (20 μM) (15). Taking the experimental error and the error from Scatchard plot into account, the two results are in good agreement for intact PSII. It is noteworthy that the parameters obtained from the multiphasic Scatchard plot are an estimate, and only the total number of binding sites can be deduced by simply extrapolating the curve to find the x-intercept. Here the plot in Figure 19 was decomposed as described in (51) and this approach gives a minimal picture of the features of the system.

CHAPTER V

RESULTS AND DISCUSSION: ANION EFFECTS ON THE S_2' STATE

The OEC cycles through five redox states denoted S_0 to S_4. EPR signals have been detected from all S states, except the S_4 state. The S_2 state is characterized by the extensively studied multiline signal at g = 2 and the alternative g = 4.1 signal (35). The S_3 state was characterized by recently discovered integer spin signals at g = 12 and 8 (52). Interestingly, the S_3 state was found to be sensitive to near-infrared (NIR) light. NIR excitation of the S_3 state produced prominent EPR signals at about g = 4.7 and g ~3, which have been assigned to an intermediate state, denoted the S_2' state (44). The S_2' state was associated with a proton-deficient S_2 configuration with a 7/2 spin state (40). The observation that a g = 4.7 signal was produced directly by illumination of

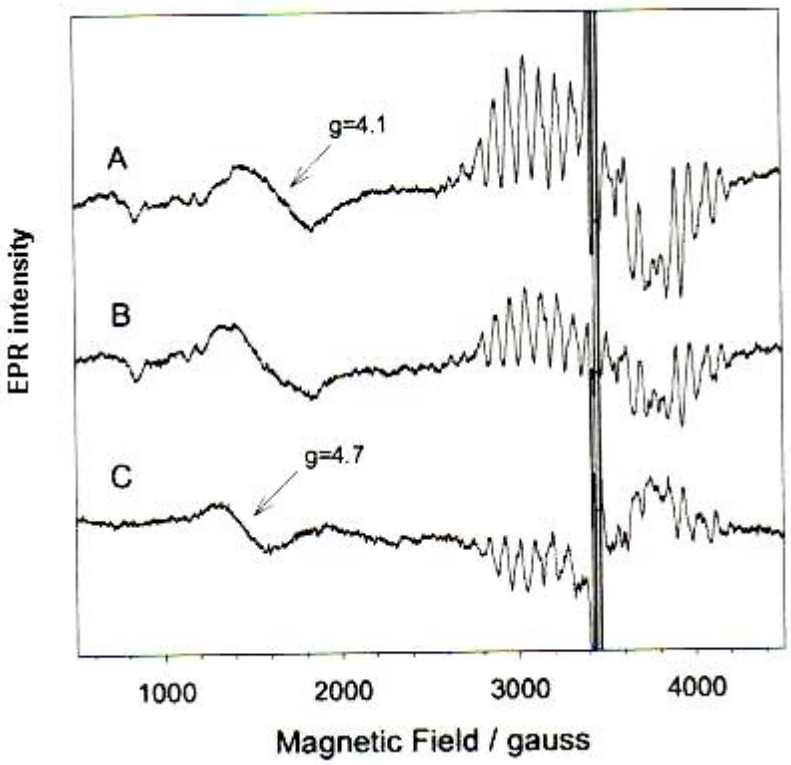

Figure 20. The production of the S_2' state by long term incubation. A: sample illuminated 6 min at 243 K minus dark spectrum
B: same sample further incubated in liquid N_2 (77 K) for 11 days minus dark spectrum
C: B minus A

the S_1 state at alkaline pH and -30ºC supported the identification of the state with deprotonation of ligands to the Mn cluster (37). The position and intensity of the g ~ 3 signal are thought to vary strongly with slight changes in the crystal field parameters (37, 40, 53).

The S_2' signal can also be produced by prolonged incubation of S_3 state at 77 K (11). This is illustrated in Figure 20. An intact PSII sample with the nonheme iron preoxidized was illuminated as described in the Materials and Methods section and thus advanced to a mixed state of S_2 and S_3 (trace A). Then the sample was incubated at 77 K in the dark for 11 days (trace B). The S_2' state signal at g = 4.7 (trace C) was obtained after subtraction of trace A from trace B. In a previous study (37, 53), only the nearly isotropic g = 4.7 signal was observed by the prolonged incubation of the S_3 state at 77 K. However in the present study, the g ~ 3 signal was also observed by 77 K incubation, either separately or concomitantly with the g = 4.7 signal (spectra shown later). According to Petrouleas and colleagues, the g = 4.7 only spectrum represents the most relax configuration of the S = 7/2 state, and the g ~ 3 signal may represent a transient configuration. This was supported by the gradual conversion of g ~ 3 signal to g = 4.7 signal at 77 K (37). Probably in the two different treatments (NIR excitation vs incubation at 77 K), the S_3 state decays through the same mechanism, resulting in the same modified S_2 configuration, S_2' state.

Chloride has been known to be required for the formation of the multiline signal of the S_2 state and for the S_2-S_3 and S_3-S_0 transitions (38, 39). Thus the removal of Cl^- may also prevent the formation of the S_2' state since it appears as a result of decay of the S_3 state. Addition of other ions (Br^-, I^-, NO_3^-) to Cl^- depleted PSII can restore the S_2 state partially. I^-, unlike the other ions, shows inhibitory effects on the

oxygen evolution activity in the presence of Cl^-. The inhibition by I^- occurs at a state higher than S_2 (41). The I^- effects on the S_2' state in the presence and absence of Cl^- were investigated in this study.

1. Time Dependence of S_2' Signal Formation

It has been reported that the S_2' state accumulated with the decay of the S_3 state during the incubation at 77 K (37). The following experiment was done to determine the optimal incubation time in both intact PSII and Cl^- depleted PSII with the readdition of Cl^-.

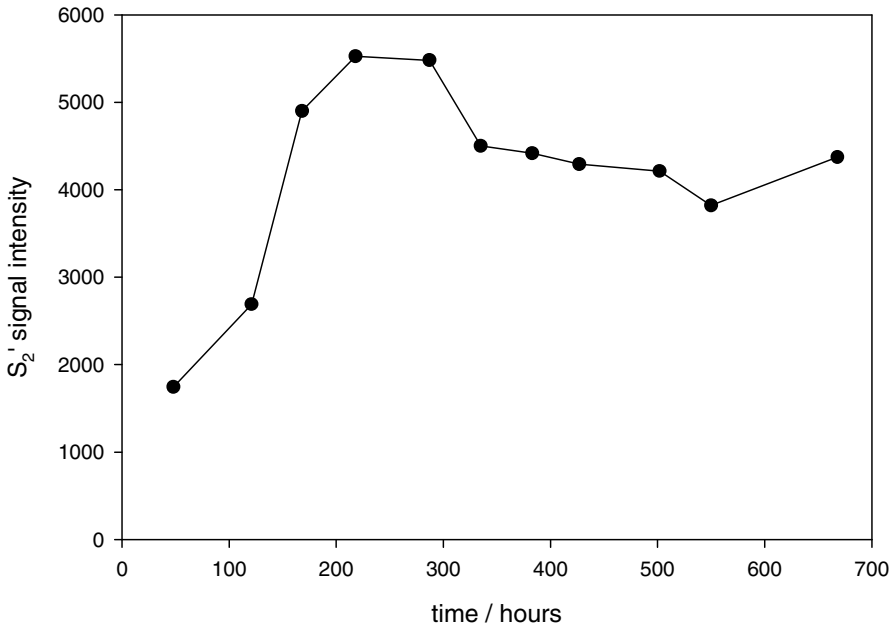

Figure 21. Time dependence of the formation of the S_2' signal at g =4.7 in intact PS II. The S_2' signal reached a maximum between 200-300 hours incubation at 77 K.

In Figure 21, intact PSII with ferricyanide treatment was advanced to the S_3 state as described in the Material and Methods section and the spectrum was

recorded. Then the sample was stored at 77 K in the dark, and spectra were collected at different time points, ranging from 48 to 668 hours. The g = 4.7 S_2' state signals at different time points were obtained by subtraction of the S_3 state spectrum from the spectra after incubation. The intensity of the S_2' signals reached a maximum between 200-300 hours incubation at 77 K. The S_2' state was fairly stable at 77 K, and after very long incubation (>600 hrs), the intensity of the S_2' state signal stayed at a relatively high level without decreasing.

A very similar pattern was observed in Cl^- depleted PSII after readdition of Cl^- (Figure 22). The intensity of the S_2' state signal became maximal after 200-250 hours incubation of the S_3 state at 77 K. Therefore the optimal incubation time for the S_2' state was 8 - 10 days for both intact PSII and Cl^- depleted PSII with added Cl^-.

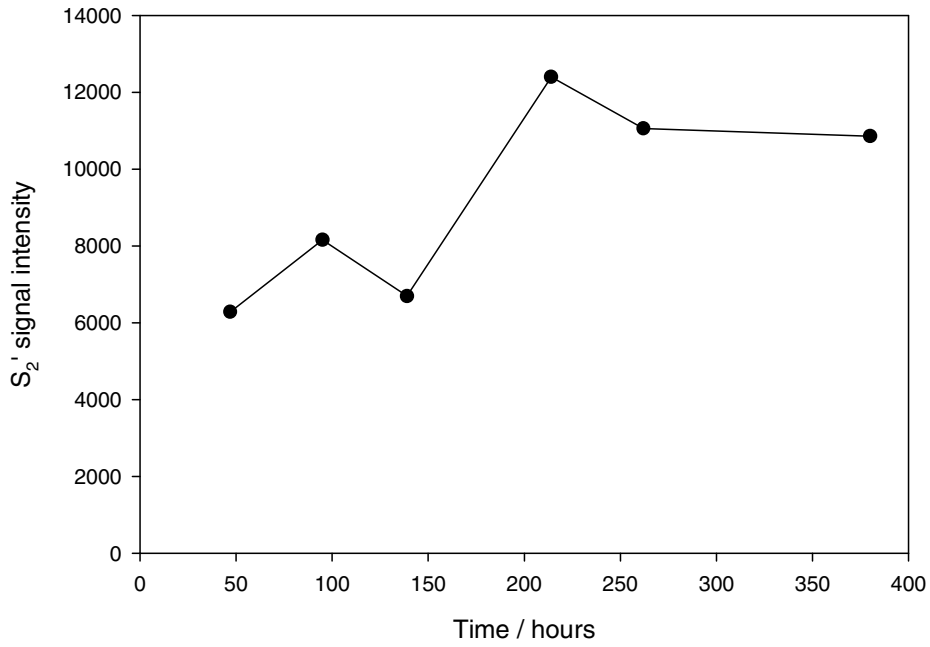

Figure 22. Time dependence of the formation of the S_2' signal at g =4.7 in Cl^- depleted PS II with added Cl^- to a concentration of 15 mM. The S_2' signal reached a maximum between 200-250 hours incubation at 77 K.

The examination of the S_2' signal was also carried out in Cl^- depleted PSII without added Cl^- and/or other anions. No S_2' signal was observed in this sample. It was found that the S_2' state can also be produced in a NaCl-washed PSII sample containing Cl^- (Figure 23). Thus it is concluded that chloride is required for the formation of the S_2' state. Chloride has been known to be necessary for the S_2-S_3 and S_3-S_0 transitions. In the Cl^- depleted sample, the S_2 state can't advance to the S_3 state upon illumination, although it induces $Q_A^-Y_Z^+$ formation and recombination (38). Since the formation of the S_2' state is correlated with the decay of the S_3 state, the S_2' state is not expected to form in the absence of chloride.

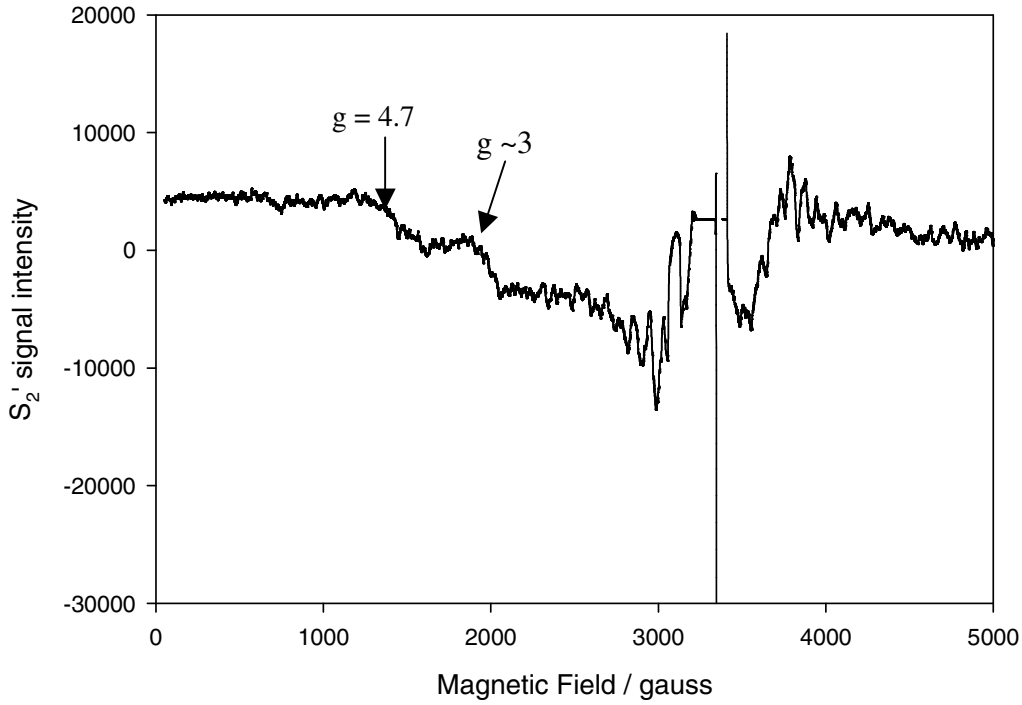

Figure 23. The S_2' state signals in NaCl-washed PSI containing 15 mM Cl^-. Both g = 4.7 and g ~ 3 signals were observed.

2. Iodide Effect on theS_2' Signals

Chloride has long been known as a cofactor required for oxygen evolution by PSII. Activating Cl^- can be replaced by several other anions (Br^-, I^-, NO_3^-, and NO_2^-) with lower efficiency. Among these anions, I^- and probably NO_2^- are special due to their dual effects on oxygen evolution activity. In the absence of Cl^-, I^- activates oxygen evolution activity at low concentrations (up to 2 mM), but shows inhibitory effects on oxygen evolution activity at high concentrations (2 ~ 25 mM) (41). In the presence of Cl^-, I^- is an inhibitor at all concentrations. Kinetic study revealed that I^- is an uncompetitive inhibitor with an inhibition constant of K_i = 37 mM, which implied that the activating Cl^- or I^- binds before the inhibitory I^- can bind. EPR spectroscopy showed that I^- at both high and low concentrations supported the formation of the S_2 state EPR signals. So the inhibition by I^- must occur at a state higher than the S_2 state. It was also concluded that I^- has two binding sites on PSII, one for activating Cl^- or I^- and another for inhibitory I^- (41).

Chloride is known to be required for the formation of the S_2' state as shown in the preceding experiment. I^- at low concentrations is expected to support the formation of the S_2' state in the absence of Cl^- since I^- substitutes for Cl^- at the activating site. If the inhibition by I^- occurs at a higher state up through the S_3 state, I^- may also inhibit the formation of the S_2' state from the second site. Alternatively if the inhibition by I^- occurs at the highest state, S_4, or an intermediate state between S_3 and S_4, then the S_2' state may be formed in the presence of high concentrations of I^-. The following experiment was performed in Cl^- depleted PSII with and without added I^- to test the hypothesis.

To investigate the effects of I^- on the S_2' signals, a series of samples with varying amounts of I^- and Cl^- were studied. Cl^- depleted PSII samples were prepared with 15 mM NaCl and no added anion as positive and negative controls, respectively. Samples were also prepared with 2 and 25 mM NaI in the absence of Cl^-. In addition, one sample was prepared with both NaCl (15 mM) and NaI (50 mM) to investigate the inhibition by I^-. In the presence of added Cl^-, the S_2' state signal at g ~ 3 was formed, whereas in the absence of any added anion, only the g = 4.1 signal was observed, which is consistent with previous observed effects of Cl^- depletion on the S_2 state (Figure 24, trace A & B). The S_2' state signal at g ~ 3 and g = 4.7 were observed in "I^- containing only" PSII samples, for both high and low concentration (Figure 24, trace C & E). Even in the presence of Cl^-, there was no obvious inhibition

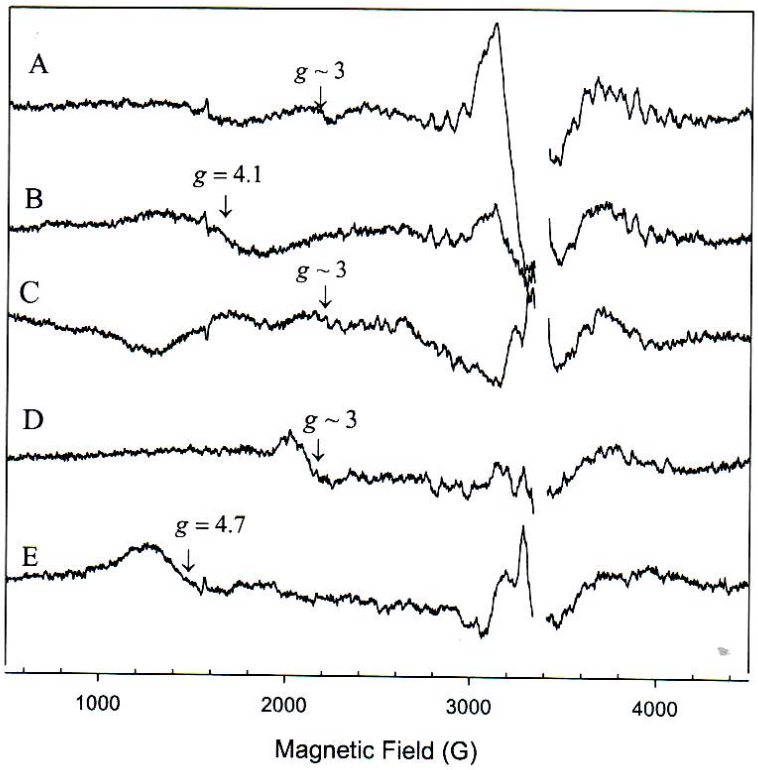

Figure 24. S_2' state spectra of Cl^- depleted PS II resupplied with chloride and iodide. The anions were provided as the sodium salt. Spectra were obtained after 9 days incubation at 77 K.
A: 15 mM Cl^-; B: no anion added; C: 2 mM I^-; D: 15 mM Cl^- and 50 mM I^-; E: 25 mM I^-. Sample preparation and EPR spectroscopy were carried out as described in Materials and Methods.

due to I^-, since the S_2' state signal at g ~ 3 was observed (Figure 24, trace D). Quantification of the signals could not be made in this situation because of the high error in signal heights and because the two S_2' state signals were not observed simultaneously in any one spectrum. However we can conclude that I^- can promote formation of the S_2' state at both high and low concentrations and in the presence and absence of Cl^-. This indicates that the inhibition by I^- occurred at a state higher than the S_2' state. No S_2' state signal was observed in the absence of any anion, indicating that I^- substituted for Cl^- at the Cl^- activating binding site for formation of the S_2' state.

Of the two I^- binding sites on PSII, one is associated with activation of oxygen evolution, a role which is normally filled by Cl^-. The functional role for the second I^- binding site, which is associated with inhibition, is not clear so far. The recent crystal structure of PSII revealed that the OEC has the capacity for multiple binding sites for water and ions (12). Previous research (37, 40, 53) and the study presented here have shown that the S_2' state is produced by the decay of the S_3 state through incubation at 77 K or NIR excitation of the S_3 state at 50 K. Presumably, I^- did not inhibit the formation of the S_3 state and the inhibition by I^- occurred at a state higher than the S_3 state. One possibility is that the inhibitory I^- blocked the water or hydroxyl ion binding at the S_3 state or a state higher than S_3. Another possibility is that the second I^- binding site is an anion site that facilitates the binding and exchange of Cl^- at its site of activation (41). Previous researchers have pointed out that the second I^- site is located in close proximity to Tyr Z of the OEC and may be normally occupied by water or hydroxyl ion (41). The possibility that the S_4 state is formally equivalent to $S_3 + Y_Z^{\cdot}$ was suggested based on the observation that oxygen release and the final

electron transfer out of the OEC occur on the same 1 ms timescale (2). I^- could possibly be oxidized by the radical Y_z in the S_4 state, thereby resulting in the iodination of the protein D1 and damage to the PSII, therefore inhibiting oxygen evolution activity.

The production of the S_2' state by the straightforward illumination of the S_1 state at -30 ºC at alkaline pH was accompanied by the formation of a g ~ 5 signal, which supported the suggestion that the S_2' state is a proton deficient configuration of the S_2 state (37). The formation of the S_2' state in this case appeared not to require the decay of the S_3 state, but rather was attributed to the deprotonation of the S_2 state. In another study, the alkaline treatment of PSII was found to decrease the multiline signal of the S_2 state and inhibit the S_3-S_4 transition (54). The effect of I^- on the S_2' state at alkaline pH would be an interesting area of future study.

CHAPTER VI

CONCLUSION

In summary, we confirmed that one PSII unit contains one Cl^- trapped by the 17 and 23 kDa subunits based on a simple analysis, although the Cl^- content in Cl^- depleted PSII remains further investigation. The EPR study of the S_2' state of PSII suggested that Cl^- is necessary for the formation of the S_2' state and that the inhibition by I^- occurs at a state higher than the S_2' state.

Lindberg *et al*. have reported that a high-affinity slow exchanging binding site for chloride is present in PSII. They determined that the amount of chloride in this site is 1 Cl^-/PSII using radioactive ^{36}Cl-labeled PSII (15, 46). No other Cl^- measurement in PSII was done before on a routine basis because of the difficulty in pretreatment of the sample, the presence of background contaminating Cl^-, and the high detection limit of methods available. In the present study, the attempts that were made to wet ash the PSII membranes and then measure Cl^- content by the AgCl colloid assay turned to be unsuccessful due to the high background from the PSII membrane proteins themselves and the additional dilution factor introduced by the bleach step. In addition, the fairly high concentration of acid needed to ash the PSII membrane and followed by the large amount of base (NaOH) added to neutralize the sample resulted in a high concentration of electrolyte in the samples, which was probably responsible for the coagulation of AgCl.

To avoid the above problem, Cl^- in PSII membranes was released using sulfate treatment at pH 7.5 and separated from the PSII membranes by centrifugation.

The 17 and 23 kDa proteins and any chloride they retained was removed from PSII membranes very rapidly (15 min) by this treatment (38, 47). After centrifugation, chloride stayed in the supernatant, which was a relatively simple system containing only the 17 and 23 kDa proteins plus buffer media. Then the Cl^- content was determined by AgCl colloid assay without the interference from the complicated PSII membrane proteins and the high amount of electrolytes. However the Cl^- content in the supernatant was very low (μM range), so it was critical to keep the chloride contamination as low as possible. The concentration of contaminating Cl^- in the buffer media was therefore controlled below 1 μM. Assuming that all high affinity bound Cl^- was released from PSII by sulfate treatment, we determined 1 Cl^-/PSII, which was consistent with Lindberg's result.

Whether chloride is necessary for oxygen evolution is under debate. Cl^- depleted PSII still retained 30-40 % oxygen evolution activity (15), suggesting that Cl^- is not required for oxygen evolution. Conversely, NaCl-washed PSII in which Cl^- is not retained by the 17 and 23 kDa subunits loses almost all oxygen evolution activity, strongly suggesting that Cl^- is necessary for oxygen evolution. Accurate measurement of Cl^- content in both Cl^- depleted and NaCl-washed PSII can resolve this question. Unfortunately, the currently available methods in our lab including AgCl colloid assay and Cl^- sensitive microelectrode were not sensitive enough to detect such trace amounts of Cl^- in both Cl^- depleted and NaCl-washed PSII directly. Chloride is also very difficult to determine via Inductively Coupled Plasma Mass Specetrometry (ICP-MS) because the ions formed by the ICP discharge are typically positive ions, whereas chlorine prefers to form negative ions. Ion chromatography has been used to analyze halogens efficiently and the detection limit can be as low as 0.01

mg/l. So ion chromatography may be a good choice to detect trace amount of Cl^- in PSII in future studies.

The study of chloride binding affinity in NaCl-washed PSII revealed two classes of binding sites with dissociation constants of 53 μM and 4.2 mM respectively. The extremely large number of binding sites indicated a large amount of non-specifically bound Cl^- in PSII membranes under Cl^- sufficient conditions. It should be noted that for the Scatchard analysis, extrapolation of a line drawn through the lowest concentration points gives an overestimate of the number of high affinity binding sites, rather than the actual number, if low affinity binding is also present. Therefore the number of high affinity binding sites is probably lower than 7. Lindberg *et al.* have proposed a one-site, two states model for chloride binding in PSII (30), but the two site binding model was not ruled out. It is interesting that PSII membranes started to lose chloride when an excess of Cl^- (> 20 mM) was added. This result was coincident with a separate finding in our laboratory that excess Cl^- (> 20 mM) inhibited the oxygen evolution activity (unpublished data, by Xiaoming Li). Na^+, which was added as the counter ion of Cl^-, is known to non-competitively inhibit Cl^- binding at high concentrations (48). Furthermore at even higher concentrations, it is possible that the excess chloride caused a conformational change of the PSII, resulting in the release of sequestered chloride.

The S_2' state was produced in our lab by long term incubation of the S_3 state at 77 K. We discovered that both the g ~ 3 and g = 4.7 S_2' state signals could be produced by long term incubation, whereas previous research (37, 40, 53) reported that only the g = 4.7 signal was produced by incubation at 77 K, whereas the g ~ 3 signal was produced in addition to the g = 4.7 signal by NIR illumination. Moreover,

we found that the g ~ 3 signal could be detected either alone or along with the g = 4.7 signal. In previous studies, the g = 4.7 signal was assigned to the most "relaxed state" because the g ~3 signal was able to convert to g = 4.7 signal at 77 K (40). Very small differences in the crystal field parameters of the Mn cluster were thought to induce the different forms of the S_2' state (53). The observation of both signals (g = 4.7 and g ~ 3) via different treatments (incubation at 77 K vs NIR illumination) may imply that the decay of the S_3 state to the S_2' state proceeds through the same pathway in each case.

The study of the chloride requirement in the S_2' state indicated that Cl^- is necessary for formation of the S_2' state. I^-, in the absence of Cl^-, can substitute for Cl^- to promote the formation of the S_2' state at both high and low concentrations. It has been known that in the presence of Cl^-, I^- inhibits oxygen evolution activity at all concentrations, and that the inhibition by I^- only occurs at high concentrations (> 2 mM) in the absence of Cl^-. PSII membranes appear to have two I^- binding sites: one for activating oxygen evolution, another for inhibiting (41).

Even in the presence of Cl^-, I^- did not inhibit the formation of the S_2' state, indicating that the inhibition by I^-occurred at a state higher than the S_2' state. Since the S_2' state is the decay product of the S_3 state, I^- probably did not inhibit the formation of the S_3 state. It is therefore suspected that the inhibition by I^- occurs at the S_3 state or above.

The S_3-to-S_4 (S_0) transition time is relatively long (1ms). So it is possible that inhibitory I^- acts after the S_3 state is formed or at an intermediate state between the S_3 and S_4 (S_0) states. The consideration that I^- occupies the water or hydroxyl ion binding site (41) suggests that water may bind after the S_3 state is formed, although

the possibility that I^- displaced water at an earlier state can not be ruled out. Hillier and Wydrzynski have reported that a "slow" exchanging substrate-water molecule is bound throughout the entire S state cycle and a "fast" exchanging substrate-water molecule enters the reaction center after the formation of the S_3 state (55, 56). However the authors reported that the two substrate-water molecules were bound to the S_2 state in a following paper (57). Certainly, the water binding state of PSII is still under debate. Another interpretation of the inhibitory effect of I^- is that I^- may be oxidized by $Y_z^{\cdot}$. The OEC is more positively charged in the S_3 state, and the variation of charge on the Mn cluster is expected to affect the oxidation/reduction potential of Tyr Z. The oxidation potential of $Y_z^{\cdot}$ could be high enough to oxidize I^-, thereby inhibiting water oxidation.

REFERENCES

1. Szalai, V. A. & Brudvig, G. W. (1998) *American Scientist 86*, 542-551.
2. Britt, R. D.(1996) In Ort, D. R. & Yocum, C. F.(ed) *Oxgenic Photosynthesis: The Light Reaction,* PP.137-164. Kluwer Academic Publishers, Dordrecht
3. Jon Nield' website, hotsted by Dept. of Biological Science at Imperial College London, SW7 2AZ, United Kingdom.
   http://www.bio.ic.ac.uk/research/barber/psIIimages/PSII.html
   http://www.bio.ic.ac.uk/research/nield/psIIimages/PSIIsubunits.html
4. Rutherford, A. W. and Boussac, A. (2003) *Science 303*,1782-1784
5. Bricker, T. M. & Frankel, L. K. (2002) *Photosynthesis research 72*, 131-146.
6. Bricker, T. M. & Frankel, L. K. (2003) *Biochemstry 42 (7),* 2056-2061.
7. Miyao, M & Murata, N. (1984) *FEBS lett. 170*, 350-354.
8. Ghanotakis, D. F., Babcock, G. T., & Yocum, C. F. (1984) *FEBS lett. 167*, 127-130.
9. Andersson, B., Critchley, C., Ryrie, I., & Jannson, C. (1984) *FEBS lett. 168*, 113-117.
10. Kok, B., Forbush, B., & McGloin, M. (1970) *Photochem. Photobiol. 11*, 457-475.
11. Jonathan H. A. Nugent, Sandra Turconi, & Michael C. W. Evans, (1997) *Biochemistry 36*, 7086-7096
12. Ferreira, K. N., Iverson, T. M., Maghlaoui, K., Barber, J., and Iwata, S. (2004) *Science 303*, 1831-1838.

13. Rutherford, A. W. & Boussac, A. (2004) *Science 303*, 1782-1784

14. Olesen, K & Andréasson, L. E. (2003) *Biochemistry 42 (7)*, 2025-2035.

15. Lindberg, K., Vänngård, T. and Andréasson, L. E. (1993) *Photosynthesis Research 38*, 401-408.

16. Wincencjusz, H., Yocum, C. F., & van Gorkom, H. J. (1998) *Biochemistry 3*7, 8595-8604

17. Wertz, J. E. & Bolton, J. R. (1972) "Electron spin resonance elementary theory and practical applications" pp 45, 47, 50, McGraw-Hill Book Company.

18. Miller, A. F. & Brudvig, G. W. (1991) *Biochimica et Biophysica Acta 1056*, 1-18

19. Butler, W. L, Visser, J. W. M., and Simmons, H. L (1973) *Biochim. Biophys. Acta 292*, 140-151

20. Thompson, L. K., and Brudvig, G. W. (1988) *Biochemistry* **27**, 6653-6658

21. Hanley, J., Deligiannakis, Y., Pascal, A., Faller, P., and Rutherford, A. W. (1999) *Biochemistry* 38, 8189-8195.

22. Hansson Ö, Aasa R and Vänngård T (1987) *Biophys. J. 51*, 825-832.

23. Haddy, A., W. R. Dunham, R. H. Sands, and R. Aasa. (1992) *Biochim. Biophys. Acta. 1099*, 25-34.

24. Haddy, A., K. V. Lakshmi, G. W. Brudvig, and H. A. Frank (2004) *Biophys. J. 87*, 2885-2896.

25. Bonvoisin, J., Blondin, G., Girerd, JJ., & Zimmermann, JL. (1992) *Biophys. J. 61*, 1076-1086.

26. Kusunoki, M. (1992) *Chem Phys Lett 197*, 108-116.

27. Zheng, M and Dismukes, GC (1992) Murata N (ed) *Research in Photosynthesis,* pp 305-308. Kluwer Academic Publishers, Dordrecht.

28. Boussac A, Zimmermann JL and Rutherford AW (1989) *Biochemistry 28*, 8984-8989.

29. Boussac A and Rutherford AW (1988) *Biochemistry 27*, 3476-3483.

30. Lindberg, K., & Andréasson, L. E. (1996) *Biochemistry 35*, 14259-14267.

31. Ono, T. A., Hakayama, H., Gleite, H., Inoue, Y., and Kawamori, A. (1987) *Archives of Biochemistry and Biophysics 256*, 618-624.

32. Yachandra, V. K., Guiles, R. D., Sauer, K., and Klein, M. P. (1986) *Biochimica et Biophysica Acta 850*, 333-342.

33. Haddy, A., Kimel, R. A., and Thomas, R. (2000) *Photosynthesis Research 63*, 35-45.

34. Ono, T., Zimmermann, J. L., Inoue, Y., and Rutherford, S. W. (1986) *Biochimica et Biophysica Acta 851*, 193-201.

35. Casey, J. L., and K. Sauer. (1984) *Biochim. Biophys. Acta. 767*, 21-28

36. DeRose VJ, Latimer MJ, Zimmermann JL, Mukerji I, Yachandra VK, Sauer K and Klein MP (1995) *Chem. Phys. 194*, 443-459.

37. Ioannidis, N. & Petrouleas, V. (2002) *Biochemistry 41*, 9580-9588.

38. Wincencjusz, H., Gorkom, H. V., & Yocum, C. F. (1997) *Biochemistry 36*, 3663-3670.

39. Wincencjusz, H., Yocum, C. and van Gorkom, H. J. (1999) *Biochemistry 38*, 3719-3725.

40. Sanakis, Y., Ioannidis, N., Sioros, G. and Petrouleas, V. (2001) *J. Am. Chem. Soc. 123*, 10766-10767.

41. Bryson, D., Doctor, N., Johnson, R., Baranov, S., and Haddy, A. (2005) *Biochemistry 44* (19); 7354-7360.

42. Berthold, D.A., Babcock. G.T. and Yocum, C.F. (1981) *FEBS Lett. 134*, 231-234.

43. Segel, Irwin H. (1975) in *Enzyme Kinetics Behavior and Analysis of Rapid Equilibrium and Steady-State Enzyme Systems*, pp.218-220, Wiley-interscience, New York.

44. Ioannidis, N., and Petrouleas, V. (2000) *Biochemistry 39*, 5246-5254

45. Kimura, Y., Hasegawa, K., Yamanari, T. & Ono, T-A. (2005) *Photosynthesis research 84*, 245-250.

46. Lindberg, K., Wydrzynski, T., Vänngård, T. and Andréasson, L. E. (1990) *FEBS 264*, 153-155.

47. Sandusky, P. O., Selvius DeRoo, C. L., Hicks, D. B., Yocum, C. F., Ghanotakis, D. F., & Babcock, G. T. (1983) in *The oxygen evolving system of photosynthesis* (Inoue, Y., Crofts, A. R., Fovindjee, Murate, N., Reger, G., & Satoh, K., Eds.) pp 189-200, Academic Press, Tokyo.

48. Waggoner, C., Pecoraro, V. and Yocum, C. (1989) *FEBS Lett. 244*, 237-240.

49. Waggoner, C. and Yocum, C. (1990) in *Current Research in Photosynthesis* (M. Baltscheffsky Ed.), *Vol. I*, pp 733-736, Kluwer Academic Publishers, Netherlands.

50. Miyao, M and Murata, N. (1985) *FEBS Lett. 180*, 303-308.

51. Cantor, C and Schimmel, P. (1980) in *Biophysical chemistry Part III: The behavior of biological macromolecules,* pp 856-859, W. H. Freeman and Company, New York.

52. Matsukawa, T., MIno, H., Yoneda, D., and Kawamori, A. (1999) *Biochemistry 38*, 4072-4077.

53. Petrouleas, V., Koulougliotis, D., and Ioannidis, N. (2005) *Biochemistry 44*, 6723-6728.

54. Geijer, P., Deák, Z., and Styring, S. (2000) *Biochemistry 39*, 6763-6772

55. Hillier, W., and Wydrzynski, T. (2000) *Biochemistry 39*, 4399-4405.

56. Hillier, W., Hendry, G., Burnap, R.L., and Wydrzynski, T. (2001) *J. Biol. Chem. 276*, 46917-46924.

57. Hendry, G., and Wydrzynski, T. (2002) *Biochemistry 41*, 13328-13334.